Hindawi Publishing Corporation
Journal of Nanomaterials
Volume 2014, Article ID 243041, 20 pages
http://dx.doi.org/10.1155/2014/243041

Review Article

Nanocomposite-Based Bulk Heterojunction Hybrid Solar Cells

Bich Phuong Nguyen,[1,2] Taehoon Kim,[1,2] and Chong Rae Park[1,2]

[1] *Carbon Nanomaterials Design Laboratory, Global Research Laboratory, Research Institute of Advanced Materials, Seoul National University, Seoul 151-744, Republic of Korea*
[2] *Department of Materials Science and Engineering, Seoul National University, Seoul 151-744, Republic of Korea*

Correspondence should be addressed to Chong Rae Park; crpark@snu.ac.kr

Received 30 August 2013; Accepted 20 November 2013; Published 8 January 2014

Academic Editor: Sung Jin Kim

Photovoltaic devices based on nanocomposites composed of conjugated polymers and inorganic nanocrystals show promise for the fabrication of low-cost third-generation thin film photovoltaics. In theory, hybrid solar cells can combine the advantages of the two classes of materials to potentially provide high power conversion efficiencies of up to 10%; however, certain limitations on the current within a hybrid solar cell must be overcome. Current limitations arise from incompatibilities among the various intradevice interfaces and the uncontrolled aggregation of nanocrystals during the step in which the nanocrystals are mixed into the polymer matrix. Both effects can lead to charge transfer and transport inefficiencies. This paper highlights potential strategies for resolving these obstacles and presents an outlook on the future directions of this field.

1. Introduction

Hybrid solar cells combine both organic and inorganic semiconductors in an active layer such that the organic or polymer semiconductor serves as the electron donor and transports photogenerated holes, whereas the inorganic semiconductor accepts and transports electrons [1–6]. Theoretically, the hybrid photovoltaic devices (HPVs) are expected to achieve a high power conversion efficiency (PCE) because they combine the advantageous characteristics of polymers and nanocrystals (NCs), including the flexibility, light weight, and low fabrication costs of polymer materials [7–9] and the high electron mobility, size-dependent optical properties [10, 11], and physical and chemical stability of inorganic NCs [12]. Unfortunately, the PCE values obtained thus far in hybrid devices have not exceeded 4% under simulated air mass (AM) 1.5 illumination [13]. The main barriers to a higher PCE are thought to be an inefficient exciton dissociation at the donor/acceptor (D/A) interface [14–16], inhibition of recombination [17, 18], and poor charge transport to the electrodes [19–21]. Therefore, the design of compatible surfaces, accounting for the different chemical properties of the organic and inorganic materials, and control over the phase separation of the composites are crucial for achieving rapid and high-yield charge separation at the D/A interface and for promoting charge transport and collection at the electrodes. Three distinct strategies have been explored toward improving the interface design in the nanocomposite materials to enable hybrid solar cells to achieve high PCE. The first approach, ligand exchange, uses a mix of polymers and inorganic NCs prepared via colloidal synthesis approaches. The second strategy, grafting, utilizes the grafting of a polymer from/onto the NCs, yielding polymer/NCs nanocomposites with improved grafting density. The third strategy, direct NC growth, involves the use of a molecular precursor to the inorganic semiconductor dissolved together with the polymer in a common solvent and this solution may then be used to deposit the photoactive layer.

Improving the photovoltaic efficiency requires a clear understanding of the structure-properties relationship; therefore, we focus here on one type of hybrid solar cell, hybrid bulk heterojunction solar cells. This paper provides the reader with insight into the basic principles underlying these devices and discusses the current state-of-the-art in the three synthetic strategies mentioned above. A goal in this field is to understand the crucial parameters that are responsible for HPVs performance. Motivated by the rapid growth and development of this field, this review describes the recent

advances and progress toward device improvement. An outlook is provided on the future materials and technologies that are likely to guide the future directions of research.

2. Hybrid Solar Cells

2.1. Definitions. "Hybrid" refers to the association of at least two components of distinctly different chemical natures, the molecular-level distribution of which components are achieved either through simple mixing or through linking the components together via specific interactions, such as covalent, coordination, ionic, or hydrogen bonds. Each hybrid component possesses its chemical identity and can exist independently of the hybrid material [22].

A bulk heterojunction is by definition a homogeneous blend of a p-type and an N-type semiconductor (donor/acceptor). Organic photovoltaic devices (OPVs) based on blends of conjugated polymers and fullerenes form interpenetrating donor/acceptor networks and have been used in prototype bulk heterojunction geometry applications. Bulk heterojunctions in polymer-inorganic hybrid solar cells may be formed by replacing the fullerenes, which act as organic nanoparticles (NPs), with inorganic semiconductors as electron acceptors for dispersal in the polymer matrix. NCs based on metal oxides (ZnO [23–25], TiO_2 [26–28]), group II–VI (ZnS [29, 30], ZnSe [31], CdTe [32–34], CdS [35–37]), group III–V (GaAs [38, 39], InP [40]), group IV–VI (PbSe [41], PbS [42–44]), group IV (Si [45, 46]), $CuInS_2$ [47, 48], $CuInSe_2$ [49], have been tested for their utility as electron acceptors.

2.2. Device Structure and Working Principle. NCs/polymer bulk heterojunction hybrid solar cells usually have device architecture similar to those of organic solar cells (Figure 1). Anodes are often prepared by depositing indium tin oxide (ITO), which is conductive and transparent and which displays a high work function, onto a flexible plastic or glass substrate. The conducted polymer poly(3,4-alkenedioxythiophenes):poly(styrenesulfonate) (PEDOT:PSS) provides an anode buffer material that enables efficient hole extraction. Photoactive layers may be prepared by spin-coating a NC/polymer blend solution onto an ITO substrate to form a thin film 100–200 nm thick. A top metal electrode (e.g., Al, Ag, and Ca) is then vacuum-deposited onto the photoactive layer as the cathode.

As with OPVs, the conversion of light energy into electricity takes place in four main steps: photon absorption, exciton diffusion, charge transfer, and charge carrier transport and collection (Figure 2). Both organic semiconductor materials and inorganic NCs can absorb incident light and create bound electron-hole pairs called excitons. The excitons diffuse to the D/A interface and then dissociate into free-charge carriers. The excitons dissociate at the interface if the energy levels of the NCs and the polymer are properly aligned. This charge transfer process is necessary for creating a free-charger carrier. After charge separation, the electrons and holes are transported to their respective electrodes through percolating pathways. The holes are transported through the conjugated polymer, and the electrons are transported through the inorganic semiconductor (Figure 2).

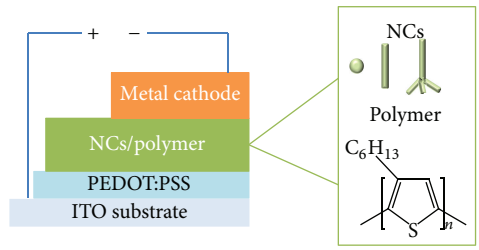

Figure 1: Schematic diagram showing the structure of a typical NC/polymer hybrid solar cell.

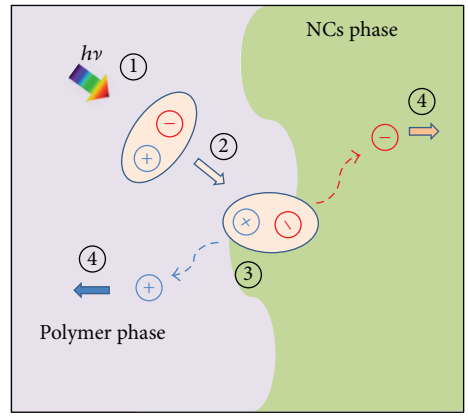

Figure 2: Schematic diagram showing the photocurrent generation mechanism in a bulk heterojunction hybrid solar cell: exciton generation (1), exciton diffusion (2), charge transfer (3), charge carrier transport, and collection (4).

The mechanism can be broken down into a number of steps, each of which may be characterized by an efficiency (η), which is defined on a scale of 0 to 1. The successful operation of a photovoltaic device requires that most or all of the steps are characterized by η close to 1. The overall efficiency of the conversion of incident photons to current, that is, the external quantum efficiency (EQE), can be written as

$$\mathrm{EQE}\,(\lambda, V) = \eta_A\,(\lambda) \times \eta_{\mathrm{diff}} \times \eta_{\mathrm{diss}}\,(V) \times \eta_{\mathrm{tr}}\,(V) \times \eta_{\mathrm{cc}}\,(V)\,, \tag{1}$$

where λ is the wavelength of the incident light and V is the voltage across the cell.

$\eta_A(\lambda)$ is the photon absorption yield. Most polymers have a bandgap larger than 2 eV, which limits the light absorption range. As such, materials with a complementary absorption spectrum in the near-infrared range [42] or ultraviolet range [57, 58] could be conjugated to the inorganic NCs.

η_{diff} is the exciton diffusion yield. The fraction of excitons that reach the D/A interface is determined by the exciton diffusion length and the location at which an exciton is created with respect to the nearest dissociation center. The exciton diffusion length in both an OPV and an HPV is in the range of 10–20 nm for a conjugated polymer [59–61].

η_{diss} is the exciton dissociation yield, which is the ratio of the number of excitons that dissociate to free charges at a D/A interface to the total number of excitons that reach the D/A interface. In a well-designed HPV, the donor and acceptor materials must have suitably been aligned with energy bands that enable exciton dissociation and provide a high overall electrochemical potential. These requirements constrain the type and range of suitable donor and acceptor materials, as well as the interactions between these materials at the D/A interface [2, 5].

η_{tr} is the charge transport yield, which is the ratio of the number of free charge carriers transported to the collecting electrode to the number of excitons dissociated at the heterojunction interface. Donor and acceptor materials are both required for a highly efficient percolated network that spans the entire active layer to provide efficient charge transport. Structural defects, impurities, and the crystallinity of both the donor and acceptor materials in the active layer can cause the charge carriers to become trapped and recombine, which reduces the transport efficiency [2]. Device architecture also require that each phase is continuous throughout the active layer to provide a pathway for rapid carrier transport to the respective electrodes.

η_{cc} is the charge collection yield. This parameter represents the ability of the charges to transfer from the photoactive layer to the electrodes. η_{cc} depends on the energy levels of the active layer and the electrode, as well as the interface properties between them [2].

A low photocurrent in an HPV results from limitations on the parameters η_{diss} and η_{tr}. Our research group has applied significant efforts toward exploiting the high internal surface area and nanoscale dimensions of inorganic/organic nanocomposites as a means for overcoming the limitations of current HPVs.

The power conversion efficiency is one of the most important parameters for characterizing the solar cell performance. Figure 3 shows a schematic diagram of the current density-voltage (J-V) characteristics of a typical hybrid solar cell in the dark and under illumination. The PCE is given by

$$\mathrm{PCE} = \frac{P_m}{P_{in}} = \frac{J_{SC} \times V_{OC} \times \mathrm{FF}}{P_{in}}, \quad (2)$$

where P_m is the maximum power point, P_{in} is the incident light density, and FF is the fill factor, which is defined as the ratio of P_m to the product of J_{SC} and V_{OC}:

$$\mathrm{FF} = \frac{P_m}{J_{SC} \times V_{OC}}. \quad (3)$$

The J_{SC} and V_{OC} are two basic factors to determine the solar cell efficiency. An understanding of the physical processes governing these two parameters is needed for the design of new materials and device configurations that would yield a high conversion efficiency [3].

J_{SC}, the short-circuit current density, depends on the incident light intensity and the absorption spectrum of the active materials. J_{SC} is given by [62]

$$J_{SC} = e \int_{E_g}^{\infty} N_{ph}(E) \times \mathrm{EQE}(E) \times dE, \quad (4)$$

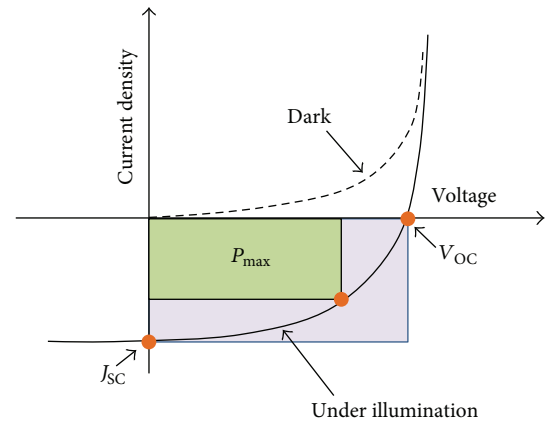

Figure 3: Current density-voltage (J-V) characteristics of a typical solar cell in the dark (dashed line) and under illumination (solid line).

where N_{ph} is the spectral photon flux of the incident light, E_g is the bandgap of the active layer, and E is the photon energy. Although inorganic acceptors can absorb light at certain wavelengths, the majority of light absorption usually takes place in the donor polymer. Dayal et al. [13] reported that the contribution of light absorption from CdSe in a poly[2,6-(4,4-bis-(2-ethylhexyl)-4H-cyclopenta[2,1-b;3,4-b′] dithiophene)-alt-4,7-(2,1,3-benzothiadiazole)] (PCPDTBT)/CdSe hybrid containing about 90 wt% CdSe nanotetrapod was only 34%. Similarly, TiO_2 and ZnO only absorb sunlight in the UV range, which is characterized by a lower photon flux than the visible or IR ranges. The calculations may therefore be simplified by assuming that light absorption only occurs in the polymer.

V_{OC} is the open-circuit voltage. V_{OC} in polymer inorganic hybrid solar cells was found to depend on the difference between the polymer's highest occupied molecular orbital (HOMO) and the inorganic acceptor conduction band [71]. Due to the quantum confinement effect, the bandgap of inorganic semiconductors varies as a function of particle size, leading to a shift in the conduction band energy level [72], which can also affect the V_{OC}. The V_{OC} of a hybrid solar cell can be increased by either moving the polymer HOMO farther away from the vacuum level or pushing the inorganic acceptor conduction band closer to the vacuum level, while retaining an energy offset between the polymer's lowest unoccupied molecular orbital (LUMO) and acceptor conduction band larger than the exciton binding energy (E_b) [3]. In a bulk heterojunction solar cell, the theoretical maximum V_{OC} can be described as

$$V_{OC,max} = E_{g,D/A} = E_{g,D} - (\mathrm{LUMO}_D - \mathrm{LUMO}_A). \quad (5)$$

The conversion efficiency may be increased by optimizing the balance between the donor gap (which mainly determines J_{SC}) and the donor conduction band (which mainly determines V_{OC}).

Table 1: Overview of hybrid solar cells prepared using nanocomposites comprising organic and inorganic materials.

Hybrid system	Aim of the work	Strategy approach	PCE (%)	Summary of findings	Reference
ITO/PEDOT : PSS/ CdSe : PCPDTBT (9 : 1 wt ratio)/LiF/Al	Characterize the properties of an HPV prepared using CdSe tetrapods and a low bandgap polymer.	Ligand exchange	3.19	Low bandgap polymers played an important role in improving the solar harvesting efficiency and the contribution of the NCs towards the PCE.	Dayal et al. (2010) [13]
ITO/PEDOT : PSS/ CdSe : PCPDTBT/Ca/Ag	Demonstrating charge transport enhancement using CdSe nanorods (NRs) and quantum dots (QDs).	Ligand exchange	3.6	A NR network in combination with small QDs produced highly interconnected pathways for electron transport within the polymer matrix. This structure enhanced charge transport and reduced recombination.	Jeltsch et al. (2012) [20]
ITO/PEDOT : PSS/ TiO_2 : MEH-PPV/Al	Characterize the properties of an HPV prepared using MEH-PPV : TiO_2 in combination with the ligands oleic acid (OA), n-octyl-phosphonic acid (OPA), or thiophene (TP).	Ligand exchange	0.157	TiO_2 capped with thiophenol yielded a higher PCE and proved to be one of the best ligands for fabricating HPVs.	Liu et al. (2008) [50]
ITO/PEDOT : PSS/ CdS : P3HT/Al	Carrier mobility enhancements could be accomplished by improving the blend interface without the use of a surfactant.	In situ growth	2.9	P3HT acts as a molecular template for CdS NC growth. The aspect ratios of CdS NRs were controlled according to the cosolvent (dichlorobenzene (DCB) and dimethyl sulfoxide (DMSO)), which induced conformational variations into the P3HT chains. Enhanced charge separation at the interface suggested electronic coupling between the P3HT and CdS components. The highly interpenetrating network increased charge transport.	Liao et al. (2009) [51]
ITO/PEDOT : PSS/ ZnO : P3HT/Al	Characterize the nanoscale P3HT : ZnO bulk heterojunction 3D morphologies using electron tomography.	In situ growth	2	The 3D exciton diffusion equation was solved, photophysical data were collected, and the 3D morphology was characterized as a function of film thickness. Charge generation and charge transport were identified as limiting the device performance.	Oosterhout et al. (2009) [52]
FTO/PEDOT : PSS/ P3HT : CdSe/P3HT/Al	A P3HT : CdSe composite was prepared using the P3HT ligand as a CdSe surface cap. The quantity of P3HT in the precursor solution was found to affect the optical properties.	In situ growth	1.32	The quantity of P3HT in the reaction did not affect the shape or phase of the CdSe superstructure samples, although it did affect the photoabsorption and photoluminescence emission intensities.	Peng et al. (2013) [53]

Table 1: Continued.

Hybrid system	Aim of the work	Strategy approach	PCE (%)	Summary of findings	Reference
ITO/PEDOT : PSS/ CdSe : P3HT/Al	HPVs were fabricated by grafting P3HT onto the CdSe nanoparticles (NPs).	Grafting	1.1	The end functional P3HT enhanced the performance of the P3HT : CdSe HPV by increasing the dispersion of CdSe without the need for a surfactant.	Liu et al. (2004) [54]
A device was fabricated using pristine ZnO, ZnO : P3HT composites and ZnO : didodecyl-quaterthiophene (QT) composites.	HPVs were prepared using P3HT and single ZnO nanowires (NWs) grafted QT	Grafting	0.036	Oligothiophene and polythiophene were grafted onto the ZnO NWs to produce p-n heterojunctions. The efficiencies of the ZnO : P3HT composites were high (0.036%) compared with the efficiencies of other devices.	Briseno et al. (2010) [55]
ITO/PEDOT : PSS/ CdS : P3HT/BCP/Mg/Ag where BCP is bathocuproine	Solvent-assisted chemical grafting and ligand exchange were used to control the P3HT/CdS interface and the CdS QD interparticle distances.	Grafting	4.1	P3HT/CdS-grafted NW structures prepared by solvent assistance (dichlorobenzene and octane) can increase the electronic interactions between the CdS QDs and the P3HT NWs. Ligand exchange reduces the distances among CdS QDs, leading to efficiently separated charge transfer.	Ren et al. (2011) [56]

3. State-of-the-Art in Hybrid Photovoltaic Materials

Bulk heterojunction hybrid solar cells lag behind the fullerene derivative-based OPVs with respect to device performance due to the limits of the current. Enhanced PCEs in bulk heterojunction HPVs may be achieved by increasing the D/A interface area, which improves the efficiency of exciton dissociation and charge transfer, and by creating interpenetrating bicontinuous percolating pathways for effective charge transport to the corresponding electrodes. Therefore, interfacial behavior and nanoscale morphology of an active layer are these critical performance factors for HPVs. Increase of D/A interface and control over the nanoscale morphology of composite layer are required; however, many issues must be overcome. First, blending inorganic NCs and organic conjugated polymers remains challenging. Dispersing inorganic NCs in a polymer matrix requires the presence of a capping agent that prevents particle aggregation but usually suppresses exciton dissociation and charge transport. Another issue is that charge transport through the composite phase is both highly sensitive to the NCs structure and to the presence of trap states within the NCs. Fortunately, significant progress toward enhancing the PCEs of HPVs has been made by optimizing colloid synthesis [73–76] and self-assembly [77, 78] procedures for preparing the NCs, as well as by tuning the shapes of the NCs (dots [79–81], rods [82–84], tetrapods [13, 85, 86], hyperbranched structures [87], wires [56], etc.). These approaches seek to prepare continuous pathways for charge transport and reduce the prevalence of carrier traps on NCs. Moreover, quantum size effects [72] may be harnessed to tune the device performance by designing the relative alignment of the energy levels in the donor and acceptor materials [84, 88].

In this review, we focus on three strategies for improving the PCE in an HPV: ligand exchange, grafting, and direct NC growth. These methods have been used to improve the polymers/NC interface properties and to control the blend morphology. The characteristics of bulk heterojunction HPV devices are summarized in Table 1.

3.1. Nanocomposites Prepared by Ligand Exchange Chemistry. Two distinct routes may be taken to produce NCs: physical approaches, in which the NCs are fabricated by lithographic methods, ion implantation, or molecular beam deposition, or chemical approaches, in which the NCs are synthesized by colloidal chemistry in solution. The unique optical and electrical properties of colloidal semiconductor NCs have attracted significant interest and have been explored in a variety of applications, such as optoelectronic devices [89], sensors [90], and photovoltaics [2, 6]. Colloidal NCs synthesized in organic media (e.g., alkyl thiol, amines, phosphines, or phosphine oxides) are usually soluble in common organic solvents

and can be mixed together with conjugated polymers, which tend to be soluble in the same solvents. Most organic surfactants and ligands tend to be insulated, which impedes charge transfer between the polymers and the NCs and impedes electron transport between adjacent NCs. In the absence of passivating ligands, it is difficult to control the composite morphology because the inorganic NCs tend to be poorly soluble in polymer matrices. The performances of such devices are significantly reduced.

In 1996, Greenham et al. investigated the effects of a QD capping ligand on the initial charge transfer process between a polymer and the CdSe QDs by simply and physically mixing the polymer and NCs [91]. By considering effective luminescence quenching as a manifestation of the exciton dissociation, these authors observed that the quenching of the photoluminescence (PL) of poly[2-methoxy-5-(2-ethylhexyloxy)-1,4-phenylenevinylene] (MEH-PPV) did not occur when 4 nm diameter CdSe NCs were capped with a long alkyl chain, such as trioctylphosphine oxide (TOPO), but that PL quenching was efficient after treatment with pyridine. The authors proposed that the lack of PL quenching was due to the ligand-covered NCs creating a barrier layer that prevented the NCs from approaching the polymer (reducing the interfacial area). The 11 Å thick TOPO alkyl barrier surrounding the CdSe NCs was sufficient to prevent charge transfer [91]. Long chain ligand-capped NCs could be exchanged with short chain ligands to enhance the interface area.

Pyridine ligand exchange is commonly used to improve the efficiency of hybrid solar cell performance. Long alkyl chain-capped NCs are generally washed with methanol several times and then refluxed in pure pyridine at the boiling point of pyridine for 24–48 h. Pyridine treatment appears to replace the insulating ligand, and the effects of pyridine exchange have been examined in the context of poly(3-hexylthiophene) (P3HT):CdSe [79, 92], PCPDTBT:CdSe [13], and MEH-PPV:CdSe [81] bulk heterojunction devices. These studies indicated that replacing the insulating ligands on the NCs with pyridine favored electron transport between NCs by reducing the insulating effects of the ligand and more intimated the contact with NCs and polymer, leading to improved J_{SC}, η_{diss}, and η_{tr}. Pyridine ligand exchange is a standard technique for preparing NPs suitable for polymer/CdSe solar cells. It is not universally suitable, however, because some polymers (such as P3HT) are not soluble in pyridine and the mechanism of ligand exchange process is still unclear [92].

The identity of the capping ligand strongly affects the degree of phase separation and the morphology of a NC/polymer thin film. A series of capping ligands (tributylamine, oleic acid, pyridine, stearic acid, and butylamine) [63, 93] have been tested in a study of their effects on the morphology and J-V characteristics of a P3HT:CdSe HPV device. The highest PCE (up to 1.8%) was obtained by using butylamine-capped CdSe NPs with a w/w mixing ratio of 12 : 1 (CdSe : P3HT) and a posttreatment temperature of 110°C. Butylamine has the advantage of providing NCs that are soluble in typical polymer solvents and of inducing the formation of a composite phase with small domains on the order of the exciton diffusion length (Figure 4). Therefore, there is considerable room for engineering ligands that can improve

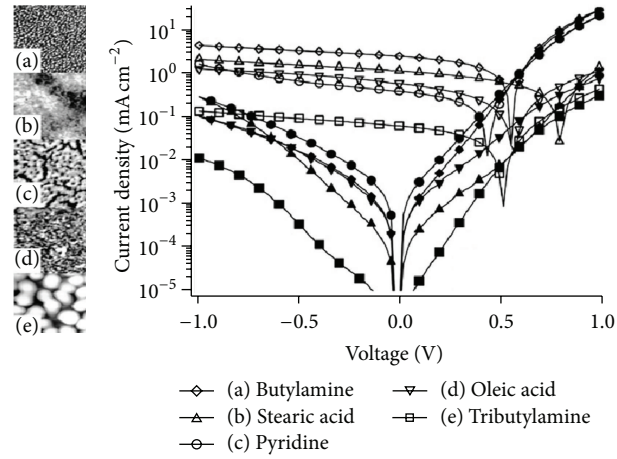

Figure 4: AFM images and J-V characteristics of CdSe NCs/P3HT films prepared using various capping ligands: (a) butylamine, (b) stearic acid, (c) pyridine, (d) oleic acid, and (e) tributylamine. Reprinted from [63] with permission from Elsevier.

exciton separation, enhance the charge transfer efficiency at the polymer/NC interface, and form percolating electron transport pathways to the cathode [94].

After ligand exchange with short chain ligand, NCs tend to aggregate and precipitate out of organic solvents, which complicate the preparation of stable mixtures of NCs and polymers. Zhou et al. applied a novel postsynthetic treatment method to spherical CdSe QDs in which the NCs were washed with hexanoic acid without inducing ligand exchange [64]. The PL quenching, TEM, and dynamic light scattering (DSL) measurements suggested that the ligand sphere had been reduced during the washing step, thereby improving the photovoltaic device efficiency (Figure 5). One advantage of this approach is that the QDs retained their solubility after acid treatment, which allows a high concentration of the CdSe QDs in P3HT (increasing η_{diss}). The large amount of CdSe led to the formation of efficient percolation networks during annealing of the photoactive composite film. Solar cells achieved efficiencies of 2.0%, which is the highest value yet reported for devices prepared using quasispherical CdSe NPs conjugated with a polymer.

Another strategy for reducing the insulating properties of the ligand in a polymer/NC hybrid material involves the application of a thermal treatment to remove weakly bound ligands [43, 65]. Seo et al. [65] replaced the TOPO ligand on CdSe NCs with tert-butyl N-(2-mercaptoethyl) carbamate ligands for the preparation of a P3HT:CdSe BHJ device by using a solvent exchange reaction. The mixture in a blend solvent was then coated onto the substrate. After heating above 200°C, the ligand was thermally cleaved with isobutene, and carbon dioxide evaporated from the film. The remaining 2-mercaptoethylamine ligands were considerably smaller than the original ligand, and the electrical characteristics of the device improved due to enhanced contact between the CdSe particles and the polymer (Figure 6). These processes increased η_{tr} and η_{diss} by forming better contact with the donor. The PCE could be increased from 0.21% to 0.44% by increasing the heat treatment temperature from 150°C to 250°C,

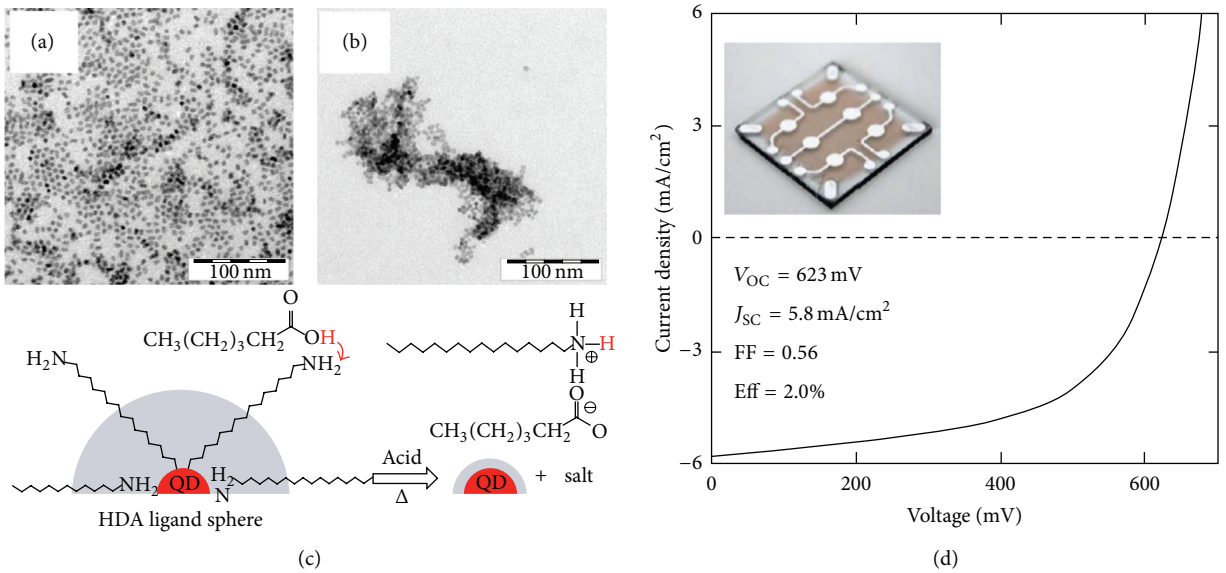

FIGURE 5: TEM images of hexadecylamine (HAD)-capped CdSe NCs before (a) and after washing with hexanoic acid (b). Proposed process for surface ligand removal (c). *J-V* characteristics of a device prepared with 87% CdSe NPs (d). Reprinted from [64] with permission from the American Institute of Physics.

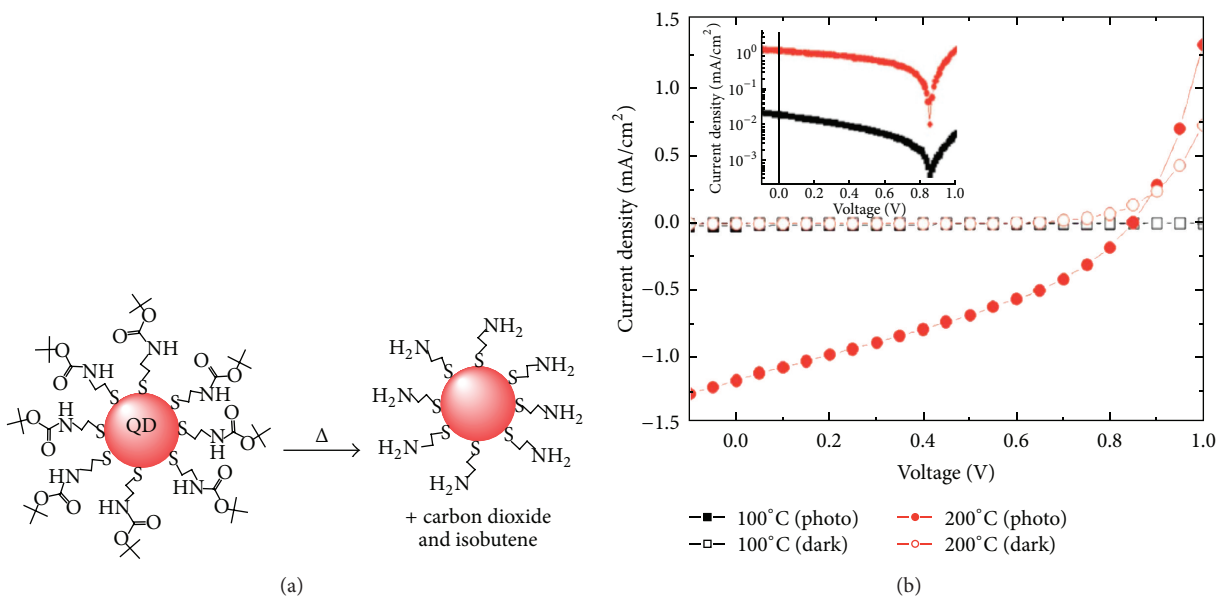

FIGURE 6: (a) Schematic illustration of the thermally induced deprotection of the tert-butyl N-(2-mercaptoethyl) carbamate ligand linked to the surface of a CdSe NC. (b) *J-V* characteristics of a device containing 90% CdSe NPs. The inset shows the photocurrent characteristics on a semilogarithmic scale. Reprinted from [65] with permission from the American Institute of Physics.

which increased J_{SC} and FF. This approach was generally less successful than the replacement of TOPO with pyridine because the glass transition temperature T_g of P3HT is below 200°C [95]. The use of ligands with a low boiling point and weak attachment properties to NCs could potentially lead to the facile preparation of multilayer devices.

The side chains of the conjugated polymers play an important role in regulating charge transfer [96]. Enhanced charge transfer at the interface of a composite may be achieved by preparing a polymer/NC blend via ligand exchange, in which the insulating capping ligand on the NC surfaces is exchanged with a functionalized polymer. This exchange process relies on the use of polymers having strongly coordinating functional groups that can anchor directly on the NC surfaces. Liu et al. prepared hybrid materials comprising NCs and a P3HT polymer matrix using an end-functional amino group [54] (Figure 7). The original surface ligands capped onto the NC surface were replaced with pyridine. The CdSe nanorods (NRs) were then mixed with either a nonfunctionalized P3HT polymer (polymer 1) or an amino end-functionalized

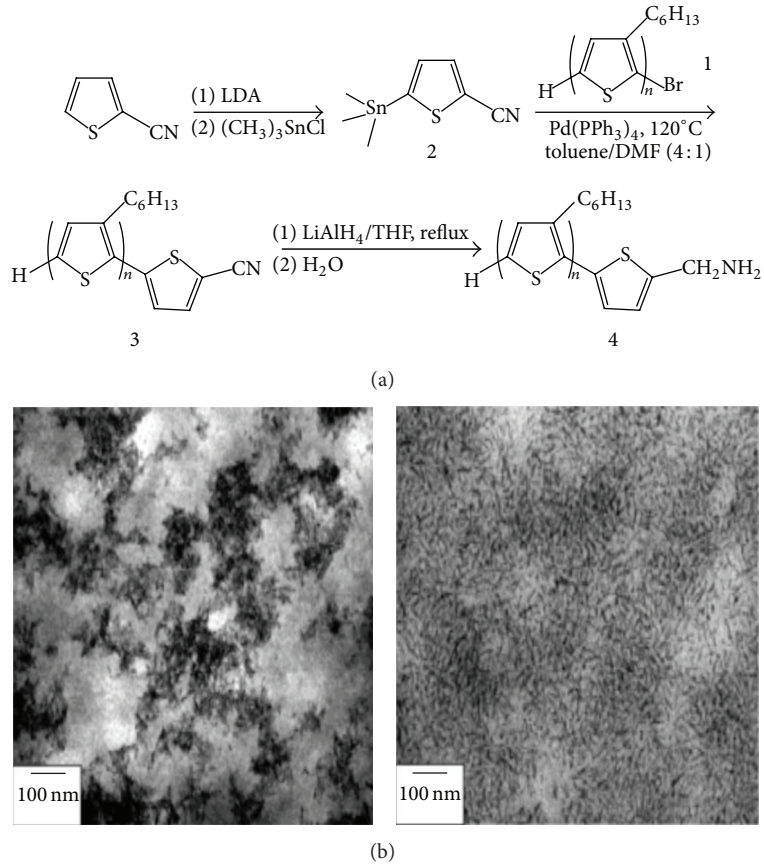

Figure 7: (a) Synthesis of P3HT using an amino end-functionalized polymer 4. (b) TEM images of CdSe (40 wt%)/polymer 1 (left) and CdSe (40 wt%)/polymer 4 (right). Reprinted with permission from [54]. Copyright 2004, ACS.

P3HT polymer (polymer 4). Interestingly, the amine-functionalized P3HT provided a PCE of 1.5%, whereas the device fabricated using the nonfunctionalized P3HT yielded a PCE of 0.5%. These results suggested that the temporary pyridine ligands were exchanged with the polymeric ligands through covalent interactions that enhanced the miscibility of the NRs in the P3HT. Chemical linkages between the polymer and the NCs offer a route to improving the NP dispersion in solvents and the electronic interactions between the polymer and NCs.

However, the amine-terminated P3HT is not a sufficiently strong functional group to fully passivate the CdSe surface capped with TOPO without the need for pyridine as an intermediate ligand. To avoid the intermediate step, which may affect the quality of the final composite material, a strong type of functional group polymer was used to directly be exchanged with the original ligand. In fact, the hybrid TOPO-capped CdSe NPs were successfully embedded in the phosphoric acid-terminated P3HT by simply mixing the components in chloroform and permitting the reaction to proceed overnight [97]. The success of bonding between P3HT and CdSe was confirmed by ^{1}H NMR. A total of 50 P3HT chains were estimated as being present on one CdSe NP, based on an analysis of the absorption spectrum. The PL quenching of the grafted P3HT and CdSe NPs clearly indicated the occurrence of charge transfer at the interface, suggesting that the electronic interactions between the functional components could be facilitated by the end-functionalizing polymers having strong binding groups.

In addition to the CdSe NCs, metal oxides, such as ZnO or TiO_2, were tested as candidate materials in green solar cell devices. TiO_2 NRs covered with TOPO ligands were synthesized for use in a hybrid solar cell. Although the PCEs of these devices were 1.14% for the pyridine ligand-capped NRs [98] or 0.03% for the dye-capped NRs [57, 99, 100], the charge separation and transport efficiency improved upon the removal of the insulating surfactant in the hybrid materials.

In 2004, Beek et al. [101] reported the performance of bulk heterojunction hybrid solar cells fabricated based on ZnO NCs and poly[2-methoxy-5-(3′,7′-dimethyloctyloxy)-1,4-phenylenevinylene] (MDMO-PPV). These cells yielded a PCE of 1.4% at AM 1.5. The ZnO NPs could be dispersed in dichloromethane, chloroform, or chlorobenzene up to a concentration of 70 mg mL^{-1} without the need for additional ligands or surfactants. However, the PCEs of the metal oxides remained low due to the presence of surface defects and large ZnO NC aggregates, which increased the recombination. Two years later, Beek et al. reported their work on ZnO NP:P3HT bulk heterojunction HPVs. The highest PCE of these devices was $\eta = 0.9\%$ [102]. The measured PCE was lower than that

obtained for MDMO-PPV:ZnO, although the hole mobility of P3HT was expected to be higher than that of MDMO-PPV. The presence of ZnO may have influenced the crystallization of P3HT because the ZnO surface was hydrophilic and the small number of ZnO clusters could not form charge transport pathways to the electrodes [103]. Many approaches to ZnO surface modification, such as using surfactants [104–106], anchoring molecules [107–109], dipolar molecules [110, 111], and dyes [112], are available to improve the dispersion of ZnO in a polymer matrix. However, surface-modified ZnO does not necessarily lead to a higher PCE because the poor phase separation can hinder charge transport. Control over particle solubility and the blend morphology remains a key requirement for improving ZnO/polymer device performances.

Further extension of the absorption spectrum into the infrared regime could be achieved using PbS or PbSe NCs. Zhang et al. [113] demonstrated HPVs based on PbS and MEH-PPV. They compared the photovoltaic performance of MEH-PPV composite device containing either OA-capped or octylmaine-capped nanocrystals after postannealing the composite layer at 220°C. The improvement in the photovoltaic performance of device using octylamine ligand-capped PbS NCs showed an 200-fold increase in J_{SC}, while devices using OA-capped NCs do not. The thermogravimetric analysis (TGA) data showed a 5% weight loss after heating to 200°C for octylamine-capped NCs, while no appreciable weight loss was observed for OA-capped NCs below 300°C. These results suggested that a certain amount of octylamine ligand is removed from the film during the annealing process (the boiling point of actylamine is 175°C), thus improving the efficiency of the charge transfer at the interface. Unfortunately, the device efficiency was very low because of the large ligand which is still surrounding the PbS NPs and unsuitable relative alignment of the energy levels in the donor and acceptor. Noone et al. [114] utilized a new polymer, poly (2,3-didecyl-quinoxaline-5,8-diyl-alt-N-octyldithieno[3,2-b:2′,3′-d]pyrrole) (PDTPQx), and the OA ligands of PbS NCs were replaced by butyl amine ligand. This device of PDTPQx:PbS (10:90 w/w) exhibited PCE of ~0.55%. More recently, the blending OA-capped PbS NCs with a low band-gap polymer, poly(2,6-(N-(1-octylnonyl)dithieno[3,2-b:20, 30-d]pyrrole)-alt-4,7-(2,1,3-benzothiadiazole)) (PDTPBT) was directly exchanged with a short length cross-linker molecule, 1,2-ethanedithiol, Seo et al. significantly improved the device efficiency to a high value of 3.78% [115].

In spite of the improvement in PbS-based hybrid solar cells, the device engineering on PbSe-based HPVs has been difficult, with a low PCE of ~0.1% to date [41]. Although the efficiency of HPVs based on PbSe is low, it has been demonstrated that Pb(Se,S) NCs based quantum dot solar cells show promising efficiency up to 7% [116, 117].

3.2. Nanocomposites Prepared via a Grafting Process. Hybrid materials may be prepared by grafting macromolecules onto NC surfaces via specially designed linker ligands containing an anchor functionality (for NC binding) and an additional reactive group capable of reacting with side- or end-functionalized macromolecules. The grafting process was realized as follows: first, the original NC surface ligands were replaced with the linker ligands; the grafting reaction was then carried out according to the reactive group type in the linker ligand and in the grafting macromolecule. An example of this process was discussed by Zhang et al. [66]. CdSe NRs were grafted to vinyl group-terminated P3HT groups via a p-bromobenzyl-di-n-octylphosphine oxide (DOPO-Br) linker group (Figure 8). In the first step, the original TOPO ligands were exchanged with pyridine. The pyridine ligands were then replaced with arylbromide-functionalized phosphine oxides. The grafting reaction was then carried out via Heck coupling between the vinyl-terminated P3HT. The solid state PL measurement of the thin nanocomposite films revealed PL quenching of the P3HT, which was indicative of charge transfer between the P3HT and CdSe NRs.

Bifunctional linker ligands have recently been tested for their utility as original NC ligands. This strategy reduces the costs and time needed for preparing hybrid materials by performing the grafting in a single step without a ligand exchange step. The bifunctional ligand (i.e., DOPO-Br) contains a phosphine oxide group at one end, similar to the phosphine group on the TOPO, which anchors the linker to the QD surface, and an arylbromide is present at the other end to enable grafting to a macromolecule [118]. CdSe QDs were grown in DOPO-Br to directly yield the DOPO-Br capped CdSe QDs. The PPV derivatives were synthesized by polymerizing 1,4-divinyl benzene with 1,4-dibromobenzene derivatives. Poly (p-phenylene vinylene) (PPV) derivatives have been directly grafted onto a DOPO-Br functionalized CdSe QD surface via Pd-catalyzed Heck coupling [67] (Figure 9). By replacing PPV derivatives, the success obtained from grafting the vinyl-terminated P3HT to the DOPO-Br functionalized CdSe QDs was expected to apply for photovoltaic devices. The end group P3HT contacted the CdSe QDs and interacted with them directly to facilitate charge transfer from the P3HT to the CdSe at the interface. PL quenching and the short fluorescence lifetime of the P3HT:CdSe composite, compared to the corresponding values obtained from P3HT alone, confirmed that the charge transfer was effective. This system suffered from some unfortunate drawbacks: the DOPO copolymerization conditions were difficult to be controlled, and this strategy cannot be extended to the synthesis of CdSe NRs because the DOPO-Br capping group is not suitable for inducing the growth of CdSe NCs.

Briseno et al. reported a convenient method for directly attaching end-functionalized polymers to NCs with bare surfaces without the need for ligand exchange and/or direct bifunctional ligand growth processes [55]. P3HT and didodecylquaterthiophene (QT), terminated with phosphonic ester and phosphonic acid, respectively, were chemically grafted onto an N-type ZnO nanowire (NW, several micrometers in length and 30–100 nm in diameter) via self-assembly of the semiconductors onto the ZnO surface in the solution phase to yield an organic shell with a thickness of about 5–20 nm (Figure 10). A single NW solar cell was successfully prepared using p-n core/shell NWs. Although the PCE of the single NW solar cell was low, 0.036%, this device permitted the isolation and study of the parameters that affect bulk hybrid solar cell performance. Increasing the P3HT layer thickness on

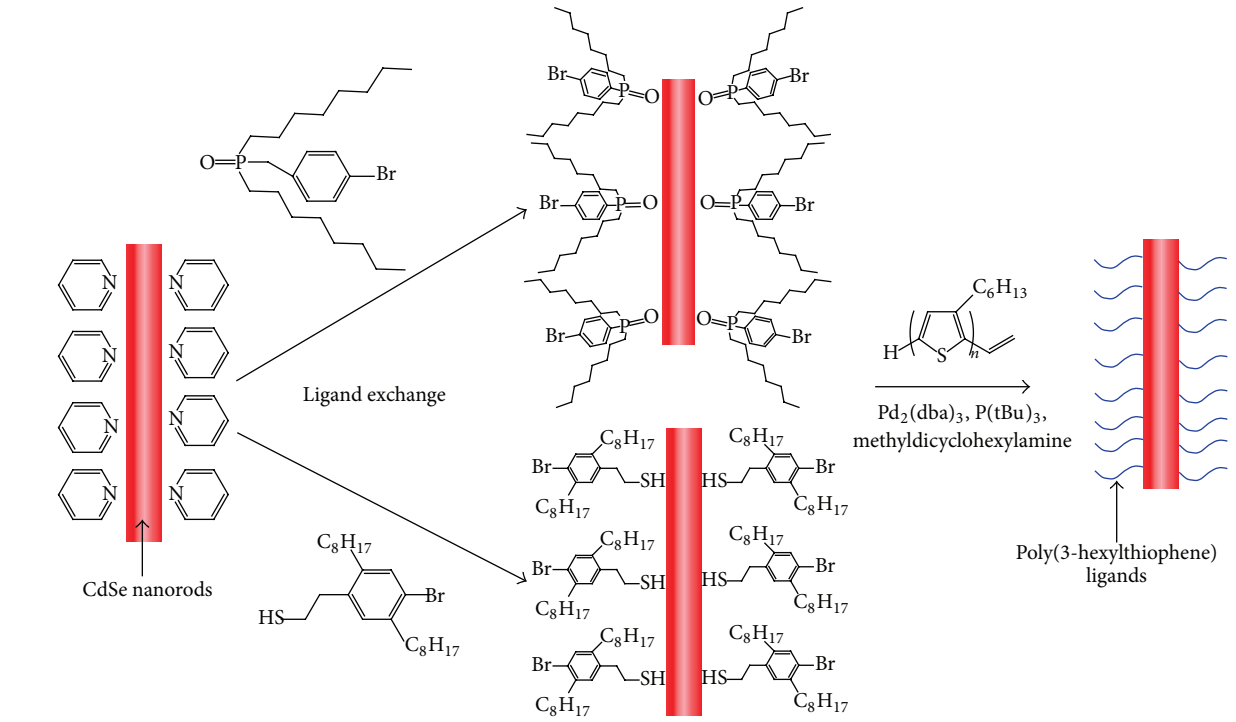

FIGURE 8: Synthesis of the P3HT-CdSe NR composites by grafting with bifunctional ligands (thiol or phosphine oxide), followed by coupling of the vinyl-terminated P3HT to the arylbromide-functionalized CdSe NRs. Reprinted with permission from [66]. Copyright 2007, ACS.

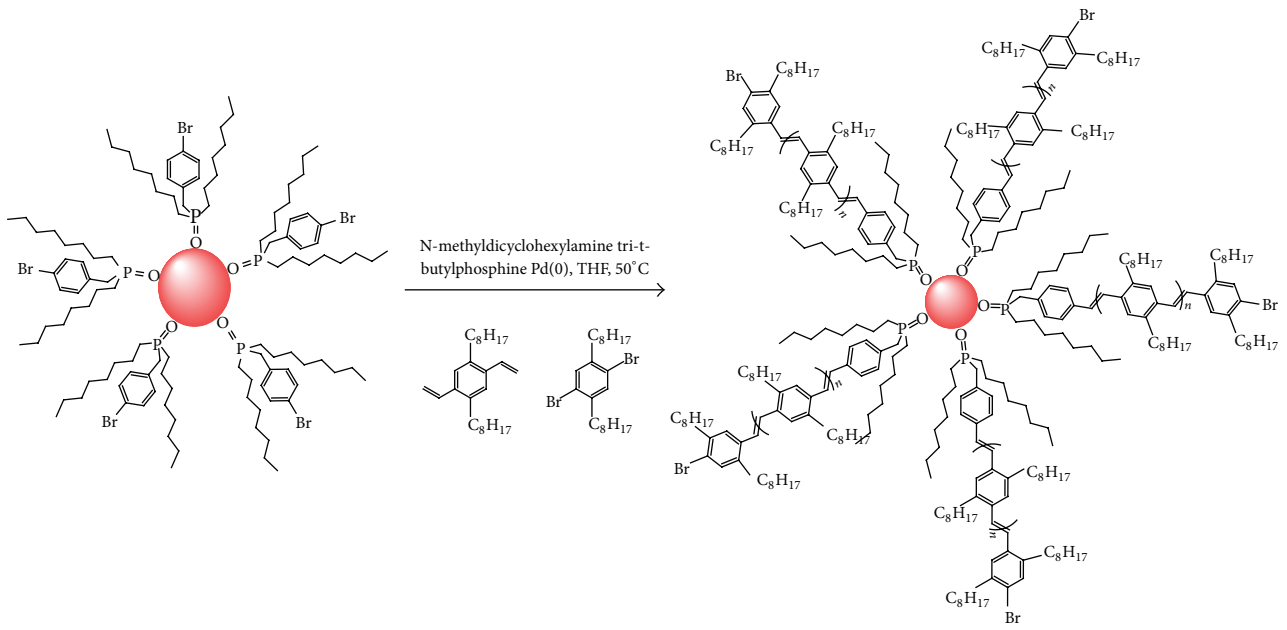

FIGURE 9: Grafting of PPV onto [(4-bromophenyl)methyl]dioctylphosphine oxide (DOPO-Br)-functionalized CdSe QDs by polymerizing from the crystal surface. Reprinted with permission from [67]. Copyright 2004, ACS.

the ZnO surface significantly improved the performance of the NW device; however, the V_{OC} in the single wire devices (V_{OC} = 0.4 V) was larger than the value reported in the literature, V_{OC} = 0.17 V for a P3HT:ZnO bulk NW array device, suggesting that the P3HT:ZnO interface in the grafted polymer was superior to the bulk spin-coated counterpart.

To date, the grafting approach offers a high grafting coverage density that increases the effective organic/inorganic interface to enable rapid charge separation. The grafting approach relies on the design of bifunctional ligands and functioned polymers that facilitate the controlled growth of NCs and the efficient grafting of NCs, respectively. However, the

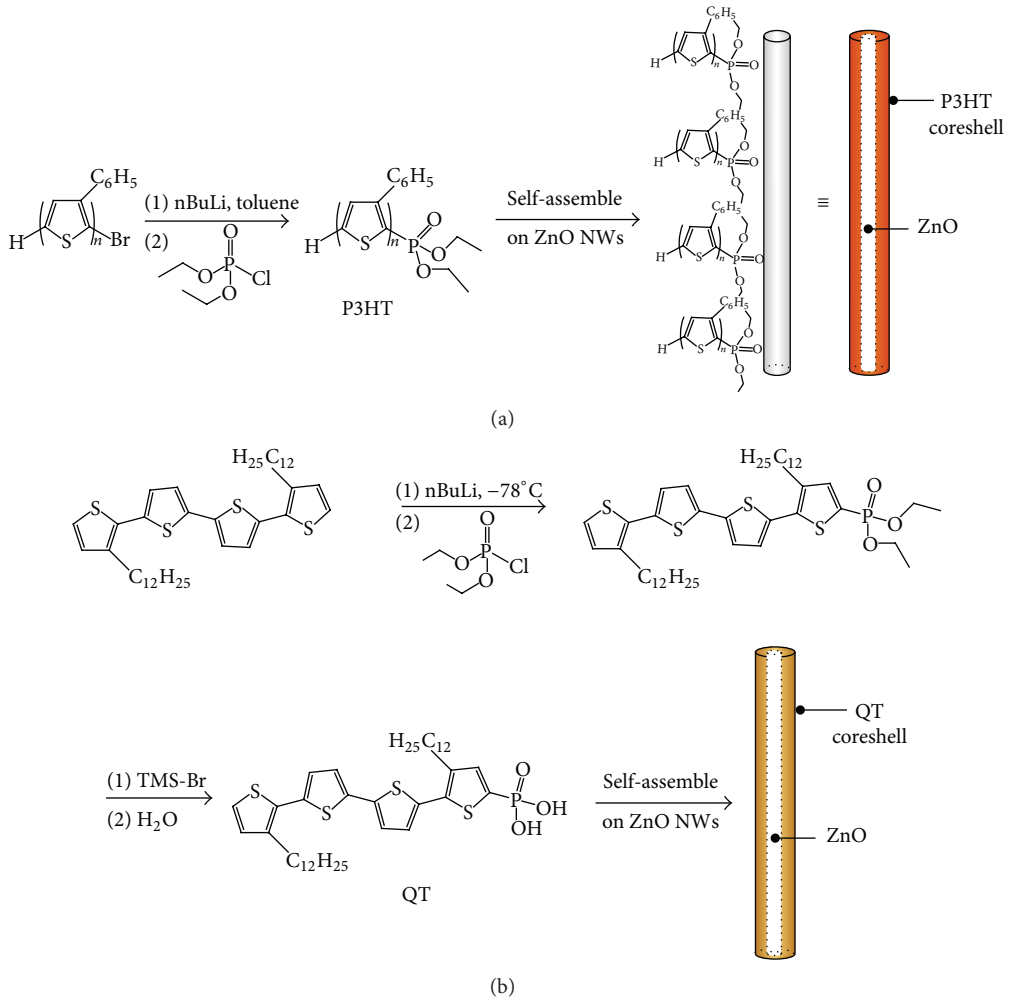

Figure 10: Synthesis of end-functionalized (a) P3HT and (b) QT bearing a phosphonic ester or a phosphonic acid, respectively. These polymers were subsequently self-assembled onto the ZnO NWs. Reprinted with permission from [55]. Copyright 2010, ACS.

surface grafting and polymerization steps are usually complicated. Excessive grafting reduces the efficiency of electron transport between adjacent NCs; thus controlling the surface grafting processes remains a challenge.

3.3. Nanocomposites Prepared via an In Situ Process. A new strategy was developed for inducing NC growth in a polymer matrix in an effort to avoid organic capping ligands and improve charge transfer between the NCs and the organic matrix. This approach relies on the dissolution of the NC precursors in a solution containing the polymer, and the NCs are then grown in the polymer template. This strategy has been applied to a variety of semiconductor NCs, including TiO_2 [119], ZnO [120, 121], PbS [44, 70], CdSe [122], and CdS [51, 69, 94].

The in situ NC growth method was first tested by preparing a TiO_2:MDMO-PPV HPV, in which titanium isopropoxide was used as the precursor. A BHJ device was expected to provide a higher efficiency than a bilayer device; however, the results of the initial test did not confirm this assumption [123]. The low efficiency of the in situ blended devices could be explained by the noncrystalline structure of the TiO_2 semiconductor. High-temperature annealing can produce crystalline TiO_2, but the high temperatures are not compatible with organic semiconductors.

This strategy was applied to the fabrication of ZnO/polymer HPVs because crystalline ZnO can be formed at low temperatures. The work of Beek et al. provides an instructive example of this approach. The photoactive layer composed of ZnO:MDMO-PPV composites was prepared by spin-coating a mixed solution containing the precursor diethylzinc and MDMO-PPV [120]. During spin-coating, diethylzinc was exposed to moisture and formed $Zn(OH)_2$ upon undergoing spontaneous hydrolysis. The thin film was then annealed at 110°C to yield an interpenetrating network of ZnO inside the MDMO-PPV. These devices offered a PCE of 1.1%, less than the value obtained for ZnO NPs mixed with MDMO-PPV (PCE = 1.6%); however, the V_{OC} reached a high voltage of 1.14 V. Such a high voltage has not previously been reported. Degradation through breakage of the transvinyl bonds in the PPV polymer upon mixing with the ZnO precursors

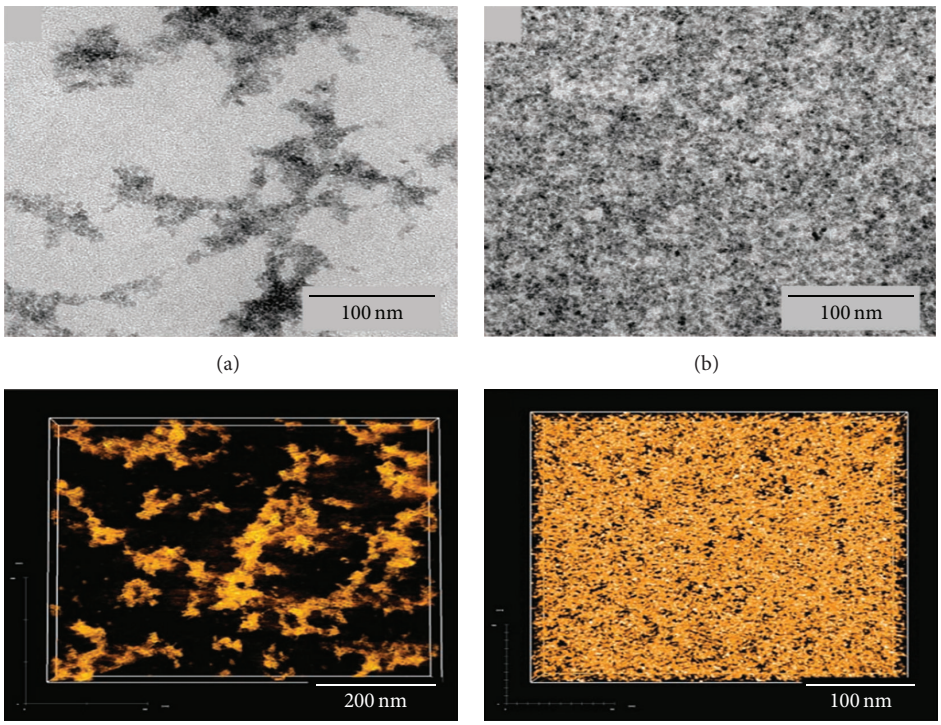

(a) (b) (c) (d)

Figure 11: TEM images of blend layers composed of ZnO:P3HT (a) or ZnO:P3HT-E (b). Reconstructed volumes based on the electron tomography of the ZnO:P3HT (c) and ZnO:P3HT-E layers (d). Reprinted from [68] with permission from Winley-VCH Verlag GmBH & Co.

produced large undesirable effects on the charge carrier [121]. The more stable P3HT did not display changes in the absorption spectra and hole transport properties during processing, providing a PCE of up to 1.4% for the ZnO:P3HT device. The improved photovoltaic performances mainly resulted from the large increase in the J_{SC}. The highest PCE yet obtained for an ZnO:P3HT HPV fabricated using this precursor method is 2% [52].

Oosterhout et al. investigated the use of an ester-functionalized P3HT-E that was more compatible toward the hydrophilic ZnO NCs [68]. The P3HT-E produced a much finer phase separation and a higher surface area upon blending with ZnO (Figure 11). J_{SC} increased due to the enhanced η_{diss} and η_{tr}; however, better mixing in the ZnO:P3HT-E composite appeared to reduce the ZnO connectivity and hole mobility in the polymer due to the lower degree of crystallinity in the P3HT-E phase. Only thin devices displayed current and PCE enhancements.

HPVs fabricated using small bandgap poly(3-hexylselenophene) (P3HS) in combination with ZnO were expected to yield a higher PCE [124]; however, the PCE of ZnO:P3HS was 0.4% due to the lower J_{SC}. The spectrally resolved external quantum efficiency was compared with the optical absorption spectrum, revealing that the amorphous P3HS regions were in direct contact with the ZnO NCs, whereas the semicrystalline P3HS phase contributed negligibly to the photocurrent. J_{SC}, therefore, decreased due to a reduction in η_{diss}. The authors indicated that the interface in ZnO:P3HS was disordered, similar to the P3HT disorder observed in ZnO:P3HT devices. The polymers rapidly degraded when mixed with diethylzinc in solution [124].

Leventis et al. introduced another in situ method for fabricating metal sulfide NP/polymer films [69]. Metal xanthate precursors were selected because they decompose at low temperatures into a metal sulfide, generating only volatile side products (e.g., H_2S, COS, C_2H_4). The decomposition process enabled the in situ growth of inorganic NCs in a relative fragile polymer host. The CdS centers formed an extended network rather than particles, which would have increased η_{tr}, had the materials not also vertically segregated, thereby reducing η_{diss} (Figure 12). The length scale of the phase segregation process depended strongly on the annealing temperature [125]. An increase in the annealing temperature from 105°C to 160°C led to a reduction in the sizes of CdS domains embedded in the P3HT matrix, from 100 nm to below 40 nm. A highly mesoporous structure formed to include interconnected CdS NP aggregates approximately 30–50 nm in diameter. The resulting photovoltaic devices exhibited a PCE of 2.17%. The in situ thermal decomposition of a single source precursor within a solid-state polymer showed promise except that aggregates formed and reduced the effective polymer/NC interface area.

Another approach to directly growing NCs involved using the polymer as a template for NC growth. The quality of the obtained NCs depended on the electrostatic and steric effects imposed by this polymer [51]. Cadmium acetate dihydrate and P3HT were dissolved in mixed solvents containing dichlorobenzene (DCB) and dimethyl sulfoxide (DMSO).

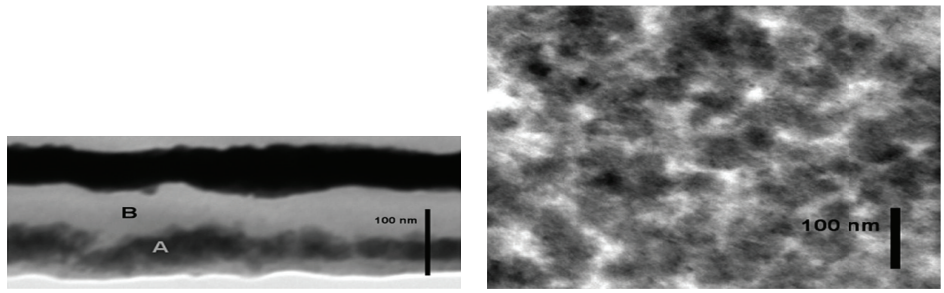

(a) (b)

Figure 12: TEM images of the CdS:P3HT composite layers. (a) TEM image of the cross section of a 2 : 1 weight ratio CdS:P3HT blend film. EDS was used to confirm the presence of Cd within region A, whereas Cd was absent from region B. (b) Top-down TEM image of a 2 : 1 weight ratio CdS:P3HT blend film. Reprinted with permission from [69]. Copyright 2010, ACS.

Sulfur in DCB solution was then injected into the conjugated polymer and precursor solution at 180°C for 30 min to form CdS NCs in the P3HT matrix. The purification of CdS/polymer composite was achieved by removing excess cadmium, sulfur ions, and DMSO via adding anhydrous methanol to form the precipitate. After centrifugation, the supernatant was then removed and the composite redissolved in DCB. The solar cells with a device architecture of ITO/PEDOT:PSS/P3HT:CdS/Al with an active layer prepared following the redissolution composite solution. In this approach, the CdS single crystal NRs having different aspect ratios were easily obtained by controlling the cosolvent mixture ratio. In fact, the cosolvent ratio could be used to modify the architecture of the polymer templates because the physical conformations of the P3HT chains were affected by the solvation properties. The planar P3HT conformation provided a stacked molecular architecture (Figure 13(a)). The Cd^{2+} ions may have been confined within the network through dipole-dipole or ion-dipole interactions between the Cd^{2+} ions and the S atoms, leading to the formation of uniformly and randomly distributed CdS NCs and NRs within the P3HT matrix. At low concentrations of the Cd^{2+} ions, CdS NRs could not be formed (Figure 13(b)), although NR morphologies started to form at higher concentrations (Figure 13(c)). Improved PL quenching was demonstrated for CdS NRs having a high aspect ratio as a result of the high interface area, which formed pathways for electron transport. A device composed of P3HT and CdS NRs with an aspect ratio of 16 showed a PCE of 2.9%.

First reports on the synthesis of PbS NCs in the solution containing a conjugated polymer were from Watt et al. in 2004 [126]. They describe the in situ preparation of PbS NCs in the presence of a conjugated polymer, either MEH-PPV [126] or P3HT [127], by heating a solution of lead acetate, elemental sulfur, and the polymer in a solvent mixture of DMSO and toluene to 160°C for 15 min. Removing excess lead and sulfur ions by precipitation and redissolution followed by coating on substrates completes the preparation of the nanocomposite layers. An advantage of this synthesis route is that size and shape of the NPs can be tuned quite easily. A controlled formation of nanosized PbS particles in the presence of the conjugated polymer was shown and attributed to steric

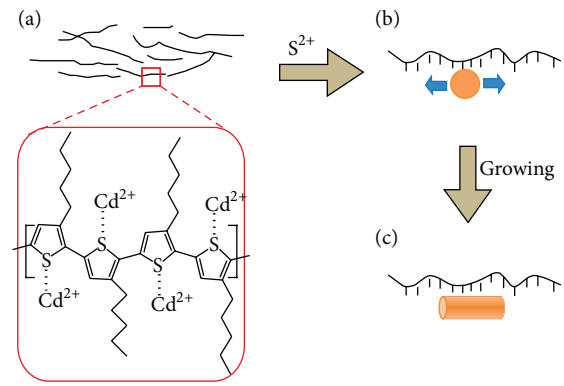

Figure 13: Schematic diagram showing the proposed CdS:P3HT composite synthesis scheme. The Cd^{2+} ions were assumed to be coupled to the unpaired S atoms along the P3HT planar chain network. Proposed mechanism for the growth of (b) CdS NCs and (d) NRs. Reprinted with permission from [51]. Copyright 2009, ACS.

effects of the long polymer chains. Without the polymer, "bulk" PbS was formed in the reaction solution. Furthermore, Stavrinadis et al. [70] showed that nanorod-like structures can be formed in a MeH-PPV matrix by a post synthetic treatment (Figure 14). A precipitation of spherical PbS NPs in MEH-PPV solution using alcohol with the appropriate polarity like ethanol, propanol, or hexanol led to dipole-induced oriented strings of PbS NPs, although a precipitation in methanol led to PbS nanocubes.

The solar cell prepared PbS NPs exhibited a V_{OC} of 1 V, an J_{SC} of 0.13 $mAcm^{-2}$, and a FF of 0.28, which leads to a PCE of 0.7% under 5 $mWcm^{-2}$ illumination [128]. The moderate I_{SC} and FF were ascribed to a high series resistance. A possible reason could have a relation large particle-particle distance of the PbS NPs.

Unlike the nanocomposites crafted by ligand exchange and direct grafting, the NC size and shape, the polymer/NCs interface, and the dynamics of NC growth in the in situ-prepared hybrid materials were complex and the interactions between the polymer and the NCs are poorly understood. The in situ approach has received significant attention due to its simplicity and its potential for producing high-efficiency

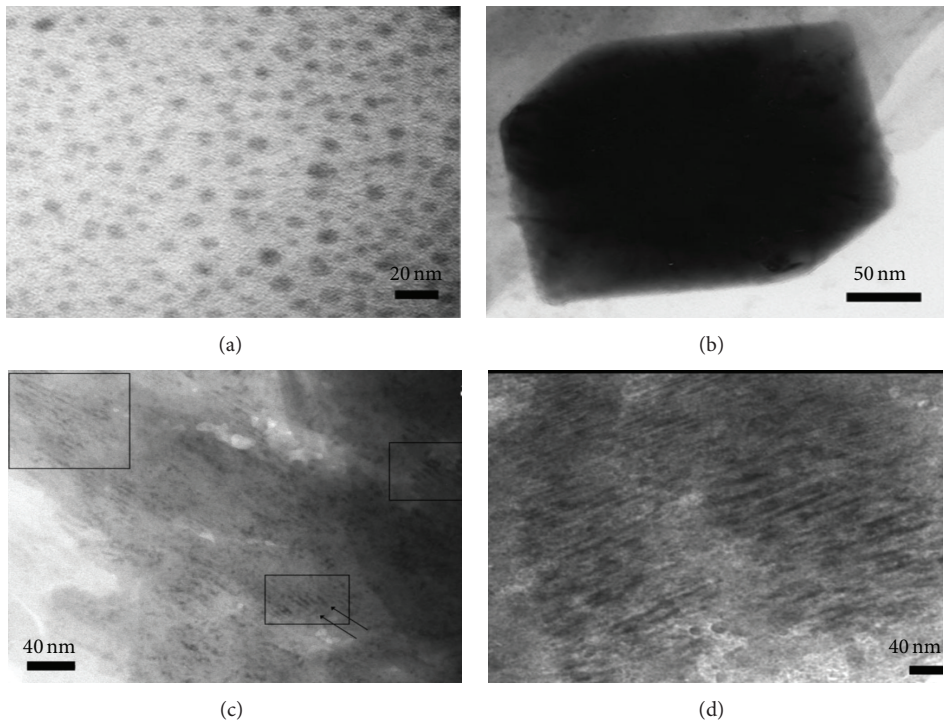

Figure 14: TEM images of PbS:MEH-PPV composites synthesis at 178°C before precipitation (a) cubic colloidal particle formed after precipitation with methanol (b) rod structure after precipitation of the 175°C composites with ethanol (c) 1-hexanol (d). The rectangles emphasize areas with clearly distinguishable nanorods. Many neighboring nanorods are aligned parallel to each other, indicated by arrows. Reprinted with permission from [70]. Copyright 2008, Winley-VCH Verlag GmBH & Co.

hybrid solar cells; however, additional work may be required to optimize the in situ growth approach.

4. Outlook and Conclusions

The polymer and inorganic components in hybrid photovoltaic devices offer complementary advantages, although the PCEs of these devices are currently low (~3.8%). The fabrication of hybrid layers that yield both a high charge generation efficiency and a high charge collection efficiency faces several challenges. The efficiency of charge generation may be improved by improving the extent of mixing between the donor and acceptor semiconductors by providing efficient exciton dissociation at the donor/acceptor interface. The controlled nanoscale morphology of the hybrid layer is required for the formation of an interpenetrating network for efficient charge transport. This review discusses three strategies for preparing HPVs: ligand exchange, grafting, and direct NC growth. These approaches are widely used to improve the compatibility of polymers and inorganic NCs of various types and dimensions in an effort to improve the photovoltaic performances of hybrid solar cells.

Modifying the surfaces of NCs or polymers is a common approach to improving the quality of the hybrid active layer in an HPV. The modifier group can help passivate the surface charge traps, suppress aggregation of the NCs in the polymer matrix, and tune the energy level offset between the semiconductor and organic layer. Nevertheless, most ligands form an insulating barrier that prevents charge transfer between the polymers and the NCs and prevents electron transport between adjacent NCs. The properties of the NC surface ligands are the principle factors limiting the efficiencies of these layers. The ligands must be removed or exchanged with more efficient surface modification molecules to improve phase separation, facilitate charge transfer, and hinder back recombination. Ligand exchange effects are not yet well understood, and precise control over certain factors, such as the exchange rate, has proven to be difficult. For the time being, the use of "small" molecules that reduce the interface surface energy has been used to replace the original ligands containing long insulating alkyl chains. The small molecules improve the efficiency of charge transfer and charge transport. For example, ZnO-modified fullerene carboxylic acid (PCBA) has been tested [108, 110]. Modifications to the ZnO NP surfaces increase the device performance from 0.59% to 1.20%. Electronic coupling between the ZnO and C_{60} derivatives increased J_{SC} to 5.39 $mAcm^{-2}$ by enhancing charge separation and improving the compatibility of the materials at the interface.

Grafting strategies are promising because they offer a high grafting density that increases charge separation. The development of controlled surface grafting processes is still needed to avoid excessive grafting, which reduces the efficiency of electron transport between adjacent NCs. Although much work can be done to optimize this approach, controlling the grafting density and the location is complicated. The use of polymer/inorganic nanocomposites blended with carbon

nanotubes (CNTs) [129–131] or graphene [132, 133] has been extremely attractive for improving the PCEs of HPVs. Semiconducting CNTs have a high absorbance in the visible and near infrared (NIR) region and a high charge mobility (up to 10^5 $cm^2V^{-1}s^{-1}$ in individual nanotubes [94]). CNTs doped or functionalized can form nano-assemblies with other molecules and polymers to provide the efficient photoinduced charge transfer or to tune the Fermi levels and to improve the positioning of the CNTs in the heterojunction region near the semiconductor [71]. In the recent study, Derbal-Habak et al. [134] demonstrated that the incorporation of 0.2% of functionalized SWCNTs into P3HT/PCBM conventional OPV improves the PCE of ~3.7%. Fortunately, Wang et al. [135] created a P3HT-PbS QDs-MWCNT nanohybrid. This device exhibited a large enhanced conversion efficiency of 3.03% as compared with 2.57% for standard P3HT:PCBM OPV. The critical role of semiconducting CNTs may improve charge transport by forming continuous pathways directly from the NCs to the electrodes that avoid the inefficient hopping pathways along the NC networks. Interestingly, a high PCE of ~14% in CNT: Si hybrid solar cells has been reported [136]. These results suggest that flexible solar cells may potentially be prepared by replacing p-type Si wafers with amorphous Si thin films.

Finally, the direct in situ growth of NCs in a polymer matrix offers an interesting approach to obtaining blends of NCs and conjugated polymers due to its simplicity and recent advances in NC synthesis. This strategy still faces several challenges. The NP size, shape, and distribution within the polymer matrix significantly influence the dielectric, electronic, optical, and structural properties of the composite layer, and the quality of NCs synthesized in situ has been rather low. This problem can be resolved by controlling the growth of NCs within the polymer matrix. A template approach employing diblock copolymers has been considered as a means for guiding the growth of NCs [137–139]. Rod-like ZnO NCs composed of ZnO NPs have been formed through templated self-assembly using a poly(3-hexylthiophene)-b-pol(zinc methacrylate acetate) (P3HT-b-PZnMAAc) diblock copolymer containing rigid thiophene chains and flexible chains [139]. The dipole-induced interactions between adjacent ZnO NPs promoted the assembly of rod-like ZnO NCs from ZnO NPs by aligning the crystal orientations and forming an interpenetrating network that offered efficient charge separation and transport. Rod-like ZnO NCs were homogeneously dispersed in the polymer matrix without the need for a surfactant, and the lengths of the rod-like ZnO NCs could be controlled by adjusting the hydrolysis time. The PCEs of the P3HT:ZnO composite devices were 0.19%, although the weight fraction of ZnO was very low (10%). A polymer having both electron accepting and electron donating building blocks has been used for the purpose of controlling the morphology in an HPV. A hybrid solar cell prepared using a liquid crystal donor/acceptor copolymer, poly[3-(6-(cyanobiphenyoxy)thiophene)-alt-4,7-(benzothiadiazole) (P3HbpT-BTD) and ZnO NPs yielded a PCE as high as 1.98% [138].

Hybrid solar cells are still lagging behind PCBM-based OPV technologies with respect to device performance and commercial applicability. HPVs are currently under development and evaluation at the basic research level, and they have the potential to undergo further significant improvements. Novel device structures, the implementation of nanostructuring methods, and the development of low bandgap materials will probably lead to PCE values on the order of 10%. Progress toward the development of organic-inorganic hybrid materials will benefit the development of hybrid solar cells as well as a variety of other applications, such as light emitting diodes, photodiodes, photodetectors, fuel cells, catalysts, and sensors.

Conflict of Interests

The authors declare that there is no conflict of interests regarding the publication of this paper.

Acknowledgments

This research was supported by the Mid-career Researcher Program and Global Research Laboratory Program through the National Research Foundation of Korea, funded by the Ministry of Science, ICT & Future Planning (No. 2010-0029244).

References

[1] B. R. Saunders, "Hybrid polymer/nanoparticle solar cells: preparation, principles and challenges," *Journal of Colloid and Interface Science*, vol. 369, no. 1, pp. 1–15, 2012.

[2] B. R. Saunders and M. L. Turner, "Nanoparticle-polymer photovoltaic cells," *Advances in Colloid and Interface Science*, vol. 138, no. 1, pp. 1–23, 2008.

[3] T. Xu and Q. Qiao, "Conjugated polymer-inorganic semiconductor hybrid solar cells," *Energy and Environmental Science*, vol. 4, no. 8, pp. 2700–2720, 2011.

[4] L. Zhao and Z. Lin, "Crafting semiconductor organic-inorganic nanocomposites via placing conjugated polymers in intimate contact with nanocrystals for hybrid solar cells," *Advanced Materials*, vol. 24, pp. 4353–4368, 2012.

[5] A. J. Moulé, L. Chang, C. Thambidurai, R. Vidu, and P. Stroeve, "Hybrid solar cells: basic principles and the role of ligands," *Journal of Materials Chemistry*, vol. 22, no. 6, pp. 2351–2368, 2012.

[6] R. Zhou and J. Xue, "Hybrid polymer-nanocrystal materials for photovoltaic applications," *Chemphyschem*, vol. 13, pp. 2471–2480, 2012.

[7] S. A. Gevorgyan, A. J. Medford, E. Bundgaard et al., "An interlaboratory stability study of roll-to-roll coated flexible polymer solar modules," *Solar Energy Materials and Solar Cells*, vol. 95, no. 5, pp. 1398–1416, 2011.

[8] F. C. Krebs, T. D. Nielsen, J. Fyenbo, M. Wadstrøm, and M. S. Pedersen, "Manufacture, integration and demonstration of polymer solar cells in a lamp for the "lighting Africa" initiative," *Energy and Environmental Science*, vol. 3, no. 5, pp. 512–525, 2010.

[9] F. Tong, K. Kim, D. Martinez et al., "Flexible organic/inorganic hybrid solar cells based on conjugated polymer and ZnO nanorod array," *Semiconductor Science and Technology*, vol. 27, Article ID 105005, 2012.

[10] C. B. Murray, D. J. Norris, and M. G. Bawendi, "Synthesis and characterization of nearly monodisperse CdE (E S, Se, Te) semiconductor nanocrystallites," *Journal of the American Chemical Society*, vol. 115, no. 19, pp. 8706–8715, 1993.

[11] T. Ling, M. Wu, and X. Du, "Template synthesis and photovoltaic application of CdS nanotube arrays," *Semiconductor Science and Technology*, vol. 27, Article ID 055017, 2012.

[12] J. Bouclé, P. Ravirajan, and J. Nelson, "Hybrid polymer-metal oxide thin films for photovoltaic applications," *Journal of Materials Chemistry*, vol. 17, no. 30, pp. 3141–3153, 2007.

[13] S. Dayal, N. Kopidakis, D. C. Olson, D. S. Ginley, and G. Rumbles, "Photovoltaic devices with a low band gap polymer and CdSe nanostructures exceeding 3% efficiency," *Nano Letters*, vol. 10, no. 1, pp. 239–242, 2010.

[14] H. Hoppe and N. S. Sariciftci, "Morphology of polymer/fullerene bulk heterojunction solar cells," *Journal of Materials Chemistry*, vol. 16, no. 1, pp. 45–61, 2006.

[15] M. Pientka, V. Dyakonov, D. Meissner et al., "Photoinduced charge transfer in composites of conjugated polymers and semiconductor nanocrystals," *Nanotechnology*, vol. 15, no. 1, pp. 163–170, 2004.

[16] E. Martínez-Ferrero, J. Albero, and E. Palomares, "Materials, nanomorphology, and interfacial charge transfer reactions in quantum dot/polymer solar cell devices," *Journal of Physical Chemistry Letters*, vol. 1, no. 20, pp. 3039–3045, 2010.

[17] M. D. Heinemann, K. Von Maydell, F. Zutz et al., "Photoinduced charge transfer and relaxation of persistent charge carriers in polymer/nanocrystal composites for applications in hybrid solar cells," *Advanced Functional Materials*, vol. 19, no. 23, pp. 3788–3795, 2009.

[18] K. M. Noone, S. Subramaniyan, Q. Zhang, G. Cao, S. A. Jenekhe, and D. S. Ginger, "Photoinduced charge transfer and polaron dynamics in polymer and hybrid photovoltaic thin films: organic vs inorganic acceptors," *Journal of Physical Chemistry C*, vol. 115, no. 49, pp. 24403–24410, 2011.

[19] D. S. Ginger and N. C. Greenham, "Charge injection and transport in films of CdSe nanocrystals," *Journal of Applied Physics*, vol. 87, no. 3, pp. 1361–1368, 2000.

[20] K. F. Jeltsch, M. Schädel, J.-B. Bonekamp et al., "Efficiency enhanced hybrid solar cells using a blend of quantum dots and nanorods," *Advanced Functional Materials*, vol. 22, no. 2, pp. 397–404, 2012.

[21] K. Kumari, S. Chand, V. D. Vankar, and V. Kumar, "Enhancement in hole current density on polarization in poly(3- hexylthiophene):cadmium selenide quantum dot nanocomposite thin films," *Applied Physics Letters*, vol. 94, no. 21, Article ID 213503, 2009.

[22] P. Reiss, E. Couderc, J. De Girolamo, and A. Pron, "Conjugated polymers/semiconductor nanocrystals hybrid materials—preparation, electrical transport properties and applications," *Nanoscale*, vol. 3, no. 2, pp. 446–489, 2011.

[23] S. R. Ferreira, R. J. Davis, Y.-J. Lee, P. Lu, and J. W. P. Hsu, "Effect of device architecture on hybrid zinc oxide nanoparticle:poly(3-hexylthiophene) blend solar cell performance and stability," *Organic Electronics*, vol. 12, no. 7, pp. 1258–1263, 2011.

[24] O. Stenzel, L. J. A. Koster, R. Thiedmann, S. D. Oosterhout, R. A. J. Janssen, and V. Schmidt, "A new approach to model-based simulation of disordered polymer blend solar cells," *Advanced Functional Materials*, vol. 22, no. 6, pp. 1236–1244, 2012.

[25] H. E. Unalan, P. Hiralal, D. Kuo, B. Parekh, G. Amaratunga, and M. Chhowalla, "Flexible organic photovoltaics from zinc oxide nanowires grown on transparent and conducting single walled carbon nanotube thin films," *Journal of Materials Chemistry*, vol. 18, no. 48, pp. 5909–5912, 2008.

[26] Y.-C. Huang, W.-C. Yen, Y.-C. Liao et al., "Band gap aligned conducting interface modifier enhances the performance of thermal stable polymer- TiO_2 nanorod solar cell," *Applied Physics Letters*, vol. 96, no. 12, Article ID 123501, 2010.

[27] S. Lu, S.-S. Sun, X. Jiang, J. Mao, T. Li, and K. Wan, "In situ 3-hexylthiophene polymerization onto surface of TiO_2 based hybrid solar cells," *Journal of Materials Science*, vol. 21, no. 7, pp. 682–686, 2010.

[28] M.-C. Wu, H.-C. Liao, H.-H. Lo et al., "Nanostructured polymer blends (P3HT/PMMA): inorganic titania hybrid photovoltaic devices," *Solar Energy Materials and Solar Cells*, vol. 93, no. 6-7, pp. 961–965, 2009.

[29] M. Bredol, K. Matras, A. Szatkowski, J. Sanetra, and A. Prodi-Schwab, "P3HT/ZnS: a new hybrid bulk heterojunction photovoltaic system with very high open circuit voltage," *Solar Energy Materials and Solar Cells*, vol. 93, no. 5, pp. 662–666, 2009.

[30] E. Maier, A. Fischereder, W. Haas et al., "Metal sulfide-polymer nanocomposite thin films prepared by a direct formation route for photovoltaic applications," *Thin Solid Films*, vol. 519, no. 13, pp. 4201–4206, 2011.

[31] D. Yun, W. Feng, H. Wu, and K. Yoshino, "Efficient conjugated polymer-ZnSe and -PbSe nanocrystals hybrid photovoltaic cells through full solar spectrum utilization," *Solar Energy Materials and Solar Cells*, vol. 93, no. 8, pp. 1208–1213, 2009.

[32] Y. Kang, N.-G. Park, and D. Kim, "Hybrid solar cells with vertically aligned CdTe nanorods and a conjugated polymer," *Applied Physics Letters*, vol. 86, no. 11, Article ID 113101, pp. 1–3, 2005.

[33] D. Verma, A. Ranga Rao, and V. Dutta, "Surfactant-free CdTe nanoparticles mixed MEH-PPV hybrid solar cell deposited by spin coating technique," *Solar Energy Materials and Solar Cells*, vol. 93, no. 9, pp. 1482–1487, 2009.

[34] H. C. Chen, C. W. Lai, I. C. Wu et al., "Enhanced performance and air stability of 3.2% hybrid solar cells: how the functional polymer and CdTe nanostructure boost the solar cell efficiency," *Advanced Materials*, vol. 23, pp. 5451–5455, 2011.

[35] H.-C. Liao, N. Chantarat, S.-Y. Chen, and C.-H. Peng, "Annealing effect on photovoltaic performance of hybrid P3HT/In-situ grown CdS nanocrystal solar cells," *Journal of the Electrochemical Society*, vol. 158, no. 7, pp. E67–E72, 2011.

[36] L. X. Reynolds, T. Lutz, S. Dowland, A. MacLachlan, S. King, and S. A. Haque, "Charge photogeneration in hybrid solar cells: a comparison between quantum dots and in situ grown CdS," *Nanoscale*, vol. 4, pp. 1561–1564, 2012.

[37] V. Resta, A. M. Laera, E. Piscopiello, M. Schioppa, and L. Tapfer, "Highly efficient precursors for direct synthesis of tailored CdS nanocrystals in organic polymers," *Journal of Physical Chemistry C*, vol. 114, no. 41, pp. 17311–17317, 2010.

[38] H. Bi and R. R. LaPierre, "A GaAs nanowire/P3HT hybrid photovoltaic device," *Nanotechnology*, vol. 20, no. 46, Article ID 465205, 2009.

[39] S. Ren, N. Zhao, S. C. Crawford, M. Tambe, V. Bulović, and S. Gradeĉak, "Heterojunction photovoltaics using GaAs nanowires and conjugated polymers," *Nano Letters*, vol. 11, no. 2, pp. 408–413, 2011.

[40] C. J. Novotny, E. T. Yu, and P. K. L. Yu, "InP nanowire/polymer hybrid photodiode," *Nano Letters*, vol. 8, no. 3, pp. 775–779, 2008.

[41] D. Cui, J. Xu, T. Zhu, G. Paradee, S. Ashok, and M. Gerhold, "Harvest of near infrared light in PbSe nanocrystal-polymer hybrid photovoltaic cells," *Applied Physics Letters*, vol. 88, no. 18, Article ID 183111, 2006.

[42] J. Seo, M. J. Cho, D. Lee, A. N. Cartwright, and P. N. Prasad, "Efficient heterojunction photovoltaic cell utilizing nanocomposites of lead sulfide nanocrystals and a low-bandgap polymer," *Advanced Materials*, vol. 23, no. 34, pp. 3984–3988, 2011.

[43] J. Seo, S. J. Kim, W. J. Kim et al., "Enhancement of the photovoltaic performance in PbS nanocrystal:P3HT hybrid composite devices by post-treatment-driven ligand exchange," *Nanotechnology*, vol. 20, no. 9, Article ID 095202, 2009.

[44] Z. Wang, S. Qu, X. Zeng et al., "Synthesis of MDMO-PPV capped PbS quantum dots and their application to solar cells," *Polymer*, vol. 49, no. 21, pp. 4647–4651, 2008.

[45] L. He, C. Jiang, H. Wang, D. Lai, and R. Rusli, "Si nanowires organic semiconductor hybrid heterojunction solar cells toward 10% efficiency," *ACS Applied Materials and Interfaces*, vol. 4, no. 3, pp. 1704–1708, 2012.

[46] C. -Y. Liu, Z. C. Holman, and U. R. Kortshagen, "Hybrid solar cells from P3HT and silicon nanocrystals," *Nano Letters*, vol. 9, no. 1, pp. 449–452, 2009.

[47] N. Radychev, D. Scheunemann, M. Kruszynska et al., "Investigation of the morphology and electrical characteristics of hybrid blends based on poly(3-hexylthiophene) and colloidal $CuInS_2$ nanocrystals of different shapes," *Organic Electronics*, vol. 13, pp. 3154–3164, 2012.

[48] E. Maier, T. Rath, W. Haas et al., "$CuInS_2$Poly(3-(ethyl-4-butanoate)thiophene) nanocomposite solar cells: preparation by an in situ formation route, performance and stability issues," *Solar Energy Materials and Solar Cells*, vol. 95, no. 5, pp. 1354–1361, 2011.

[49] E. Arici, H. Hoppe, F. Schäffler, D. Meissner, M. A. Malik, and N. S. Sariciftci, "Morphology effects in nanocrystalline $CuInSe_2$-conjugated polymer hybrid systems," *Applied Physics A*, vol. 79, no. 1, pp. 59–64, 2004.

[50] J. Liu, W. Wang, H. Yu, Z. Wu, J. Peng, and Y. Cao, "Surface ligand effects in MEH-PPV/TiO_2 hybrid solar cells," *Solar Energy Materials and Solar Cells*, vol. 92, no. 11, pp. 1403–1409, 2008.

[51] H.-C. Liao, S.-Y. Chen, and D.-M. Liu, "In-situ growing CdS single-crystal nanorods via P3HT polymer as a soft template for enhancing photovoltaic performance," *Macromolecules*, vol. 42, no. 17, pp. 6558–6563, 2009.

[52] S. D. Oosterhout, M. M. Wienk, S. S. Van Bavel et al., "The effect of three-dimensional morphology on the efficiency of hybrid polymer solar cells," *Nature Materials*, vol. 8, no. 10, pp. 818–824, 2009.

[53] Y. Peng, G. Song, X. Hu et al., "In situ synthesis of P3HT-capped CdSe superstructures and their application in solar cells," *Nanoscale Research Letters*, vol. 8, article 106, 2013.

[54] J. Liu, T. Tanaka, K. Sivula, A. P. Alivisatos, and J. M. J. Fréchet, "Employing end-functional polythiophene to control the morphology of nanocrystal—polymer composites in hybrid solar cells," *Journal of the American Chemical Society*, vol. 126, no. 21, pp. 6550–6551, 2004.

[55] A. L. Briseno, T. W. Holcombe, A. I. Boukai et al., "Oligo- and polythiophene/ZnO hybrid nanowire solar cells," *Nano Letters*, vol. 10, no. 1, pp. 334–340, 2010.

[56] S. Ren, L.-Y. Chang, S.-K. Lim et al., "Inorganic-organic hybrid solar cell: bridging quantum dots to conjugated polymer nanowires," *Nano Letters*, vol. 11, no. 9, pp. 3998–4002, 2011.

[57] Y.-Y. Lin, T.-H. Chu, S.-S. Li et al., "Interfacial nanostructuring on the performance of polymer/TiO_2 nanorod bulk heterojunction solar cells," *Journal of the American Chemical Society*, vol. 131, no. 10, pp. 3644–3649, 2009.

[58] P. V. Kamat, "Quantum dot solar cells. Semiconductor nanocrystals as light harvesters," *Journal of Physical Chemistry C*, vol. 112, no. 48, pp. 18737–18753, 2008.

[59] A. Haugeneder, M. Neges, C. Kallinger et al., "Exciton diffusion and dissociation in conjugated polymer/fullerene blends and heterostructures," *Physical Review B*, vol. 59, no. 23, pp. 15346–15351, 1999.

[60] J. E. Kroeze, T. J. Savenije, M. J. W. Vermeulen, and J. M. Warman, "Contactless determination of the photoconductivity action spectrum, exciton diffusion length, and charge separation efficiency in polythiophene-sensitized TiO_2 bilayers," *Journal of Physical Chemistry B*, vol. 107, no. 31, pp. 7696–7705, 2003.

[61] T. J. Savenije, J. M. Warman, and A. Goossens, "Visible light sensitisation of titanium dioxide using a phenylene vinylene polymer," *Chemical Physics Letters*, vol. 287, no. 1-2, pp. 148–153, 1998.

[62] T. Ameri, G. Dennler, C. Lungenschmied, and C. J. Brabec, "Organic tandem solar cells: a review," *Energy and Environmental Science*, vol. 2, no. 4, pp. 347–363, 2009.

[63] J. D. Olson, G. P. Gray, and S. A. Carter, "Optimizing hybrid photovoltaics through annealing and ligand choice," *Solar Energy Materials and Solar Cells*, vol. 93, no. 4, pp. 519–523, 2009.

[64] Y. Zhou, F. S. Riehle, Y. Yuan et al., "Improved efficiency of hybrid solar cells based on non-ligand-exchanged CdSe quantum dots and poly(3-hexylthiophene)," *Applied Physics Letters*, vol. 96, no. 1, Article ID 013304, 2010.

[65] J. Seo, W. J. Kim, S. J. Kim, K.-S. Lee, A. N. Cartwright, and P. N. Prasad, "Polymer nanocomposite photovoltaics utilizing CdSe nanocrystals capped with a thermally cleavable solubilizing ligand," *Applied Physics Letters*, vol. 94, no. 13, Article ID 133302, 2009.

[66] Q. Zhang, T. P. Russell, and T. Emrick, "Synthesis and characterization of CdSe nanorods functionalized with regioregular poly(3-hexylthiophene)," *Chemistry of Materials*, vol. 19, no. 15, pp. 3712–3716, 2007.

[67] H. Skaff, K. Sill, and T. Emrick, "Quantum dots tailored with poly(para-phenylene vinylene)," *Journal of the American Chemical Society*, vol. 126, no. 36, pp. 11322–11325, 2004.

[68] S. D. Oosterhout, L. J. A. Koster, S. S. Van Bavel et al., "Controlling the morphology and efficiency of hybrid ZnO: polythiophene solar cells via side chain functionalization," *Advanced Energy Materials*, vol. 1, no. 1, pp. 90–96, 2011.

[69] H. C. Leventis, S. P. King, A. Sudlow, M. S. Hill, K. C. Molloy, and S. A. Haque, "Nanostructured hybrid polymer? Inorganic solar cell active layers formed by controllable in situ growth of semiconducting sulfide networks," *Nano Letters*, vol. 10, no. 4, pp. 1253–1258, 2010.

[70] A. Stavrinadis, R. Beal, J. M. Smith, H. E. Assender, and A. A. R. Watt, "Direct formation of PbS nanorods in a conjugated polymer," *Advanced Materials*, vol. 20, no. 16, pp. 3105–3109, 2008.

[71] C. Goh, S. R. Scully, and M. D. McGehee, "Effects of molecular interface modification in hybrid organic-inorganic photovoltaic cells," *Journal of Applied Physics*, vol. 101, no. 11, Article ID 114503, 2007.

[72] C. B. Murray, D. J. Norris, and M. G. Bawendi, "Synthesis and characterization of nearly monodisperse CdE (E = S, Se, Te) semiconductor nanocrystallites," *Journal of the American Chemical Society*, vol. 115, no. 19, pp. 8706–8715, 1993.

[73] J. Park, J. Joo, G. K. Soon, Y. Jang, and T. Hyeon, "Synthesis of monodisperse spherical nanocrystals," *Angewandte Chemie*, vol. 46, no. 25, pp. 4630–4660, 2007.

[74] C. de Mello Donegá, P. Liljeroth, and D. Vanmaekelbergh, "Physicochemical evaluation of the hot-injection method, a synthesis route for monodisperse nanocrystals," *Small*, vol. 1, no. 12, pp. 1152–1162, 2005.

[75] X. Peng, "Mechanisms for the shape-control and shape-evolution of colloidal semiconductor nanocrystals," *Advanced Materials*, vol. 15, no. 5, pp. 459–463, 2003.

[76] H. A. Macpherson and C. R. Stoldt, "Iron pyrite nanocubes: size and shape considerations for photovoltaic application," *ACS Nano*, vol. 6, pp. 8940–8949, 2012.

[77] L.-S. Li and A. P. Alivisatos, "Semiconductor nanorod liquid crystals and their assembly on a substrate," *Advanced Materials*, vol. 15, no. 5, pp. 408–411, 2003.

[78] K. M. Ryan, A. Mastroianni, K. A. Stancil, H. Liu, and A. P. Alivisatos, "Electric-field-assisted assembly of perpendicularly oriented nanorod superlattices," *Nano Letters*, vol. 6, no. 7, pp. 1479–1482, 2006.

[79] W. U. Huynh, J. J. Dittmer, W. C. Libby, G. L. Whiting, and A. P. Alivisatos, "Controlling the morphology of nanocrystal-polymer composites for solar cells," *Advanced Functional Materials*, vol. 13, no. 1, pp. 73–79, 2003.

[80] S. Günes, N. Marjanovic, J. M. Nedeljkovic, and N. S. Sariciftci, "Photovoltaic characterization of hybrid solar cells using surface modified TiO_2 nanoparticles and poly(3-hexyl)thiophene," *Nanotechnology*, vol. 19, no. 42, Article ID 424009, 2008.

[81] L. Han, D. Qin, X. Jiang et al., "Synthesis of high quality zinc-blende CdSe nanocrystals and their application in hybrid solar cells," *Nanotechnology*, vol. 17, no. 18, pp. 4736–4742, 2006.

[82] M.-C. Wu, C.-H. Chang, H.-H. Lo et al., "Nanoscale morphology and performance of molecular-weight-dependent poly(3-hexylthiophene)/TiO_2 nanorod hybrid solar cells," *Journal of Materials Chemistry*, vol. 18, no. 34, pp. 4097–4102, 2008.

[83] B. Sun and N. C. Greenham, "Improved efficiency of photovoltaics based on CdSe nanorods and poly(3-hexylthiophene) nanofibers," *Physical Chemistry Chemical Physics*, vol. 8, no. 30, pp. 3557–3560, 2006.

[84] J. E. Brandenburg, X. Jin, M. Kruszynska et al., "Influence of particle size in hybrid solar cells composed of CdSe nanocrystals and poly(3-hexylthiophene)," *Journal of Applied Physics*, vol. 110, no. 6, Article ID 064509, 2011.

[85] Y. Zhou, Y. Li, H. Zhong et al., "Hybrid nanocrystal/polymer solar cells based on tetrapod-shaped $CdSe_xTe_{1-x}$ nanocrystals," *Nanotechnology*, vol. 17, no. 16, article no. 008, pp. 4041–4047, 2006.

[86] H. Lee, S. Kim, W.-S. Chung, K. Kim, and D. Kim, "Hybrid solar cells based on tetrapod nanocrystals: the effects of compositions and type II heterojunction on hybrid solar cell performance," *Solar Energy Materials and Solar Cells*, vol. 95, no. 2, pp. 446–452, 2011.

[87] I. Gur, N. A. Fromer, C.-P. Chen, A. G. Kanaras, and A. P. Alivisatos, "Hybrid solar cells with prescribed nanoscale morphologies based on hyperbranched semiconductor nanocrystals," *Nano Letters*, vol. 7, no. 2, pp. 409–414, 2007.

[88] J. Yang, A. Tang, R. Zhou, and J. Xue, "Effects of nanocrystal size and device aging on performance of hybrid poly(3-hexylthiophene):CdSe nanocrystal solar cells," *Solar Energy Materials and Solar Cells*, vol. 95, no. 2, pp. 476–482, 2011.

[89] S.-J. Ko, H. Choi, W. Lee et al., "Highly efficient plasmonic organic optoelectronic devices based on a conducting polymer electrode incorporated with silver nanoparticles," *Energy & Environmental Science*, vol. 6, p. 1949, 2013.

[90] R. Rajesh, T. Ahuja, and D. Kumar, "Recent progress in the development of nano-structured conducting polymers/nanocomposites for sensor applications," *Sensors and Actuators B*, vol. 136, no. 1, pp. 275–286, 2009.

[91] N. C. Greenham, X. Peng, and A. P. Alivisatos, "Charge separation and transport in conjugated-polymer/semiconductor-nanocrystal composites studied by photoluminescence quenching and photoconductivity," *Physical Review B*, vol. 54, no. 24, pp. 17628–17637, 1996.

[92] I. Lokteva, N. Radychev, F. Witt, H. Borchert, J. Parisi, and J. Kolny-Olesiak, "Surface treatment of cdse nanoparticles for application in hybrid solar cells: the effect of multiple ligand exchange with pyridine," *Journal of Physical Chemistry C*, vol. 114, no. 29, pp. 12784–12791, 2010.

[93] N. Radychev, I. Lokteva, F. Witt, J. Kolny-Olesiak, H. Borchert, and J. Parisi, "Physical origin of the impact of different nanocrystal surface modifications on the performance of CdSe/P3HT hybrid solar cells," *Journal of Physical Chemistry C*, vol. 115, no. 29, pp. 14111–14122, 2011.

[94] J. F. Lin, G. Y. Tu, C. C. Ho et al., "Molecular structure effect of pyridine-based surface ligand on the performance of P_3HT:TiO_2 hybrid solar cell," *ACS Appl Mater Interfaces*, vol. 5, pp. 1009–1016, 2013.

[95] Y. Zhao, G. Yuan, P. Roche, and M. Leclerc, "A calorimetric study of the phase transitions in poly(3-hexylthiophene)," *Polymer*, vol. 36, no. 11, pp. 2211–2214, 1995.

[96] D. S. Ginger and N. C. Greenham, "Photoinduced electron transfer from conjugated polymers to CdSe nanocrystals," *Physical Review B*, vol. 59, no. 16, pp. 10622–10629, 1999.

[97] D. J. Milliron, A. P. Alivisatos, C. Pitois, C. Edder, and J. M. J. Fréchet, "Electroactive surfactant designed to mediate electron transfer between CdSe nanocrystals and organic semiconductors," *Advanced Materials*, vol. 15, no. 1, pp. 58–61, 2003.

[98] C.-H. Chang, T.-K. Huang, Y.-T. Lin et al., "Improved charge separation and transport efficiency in poly(3- hexylthiophene)-TiO_2 nanorod bulk heterojunction solar cells," *Journal of Materials Chemistry*, vol. 18, no. 19, pp. 2201–2207, 2008.

[99] J. Bouclé, S. Chyla, M. S. P. Shaffer, J. R. Durrant, D. D. C. Bradley, and J. Nelson, "Hybrid bulk heterojunction solar cells based on blends of TiO_2 nanorods and P3HT," *Comptes Rendus Physique*, vol. 9, no. 1, pp. 110–118, 2008.

[100] J. Weickert, F. Auras, T. Bein, and L. Schmidt-Mende, "Characterization of interfacial modifiers for hybrid solar cells," *Journal of Physical Chemistry C*, vol. 115, no. 30, pp. 15081–15088, 2011.

[101] W. J. E. Beek, M. M. Wienk, and R. A. J. Janssen, "Efficient hybrid solar cells from zinc oxide nanoparticles and a conjugated polymer," *Advanced Materials*, vol. 16, no. 12, pp. 1009–1013, 2004.

[102] W. J. E. Beek, M. M. Wienk, and R. A. J. Janssen, "Hybrid solar cells from regioregular polythiophene and ZnO nanoparticles," *Advanced Functional Materials*, vol. 16, no. 8, pp. 1112–1116, 2006.

[103] P. A. C. Quist, W. J. E. Beek, M. M. Wienk, R. A. J. Janssen, T. J. Savenije, and L. D. A. Siebbeles, "Photogeneration and decay of charge carriers in hybrid bulk heterojunctions of ZnO nanoparticles and conjugated polymers," *Journal of Physical Chemistry B*, vol. 110, no. 21, pp. 10315–10321, 2006.

[104] I. Park, Y. Lim, S. Noh et al., "Enhanced photovoltaic performance of ZnO nanoparticle/poly(phenylene vinylene) hybrid

photovoltaic cells by semiconducting surfactant," *Organic Electronics*, vol. 12, no. 3, pp. 424–428, 2011.

[105] H.-P. Fang, I.-H. Chiang, C.-W. Chu, C.-C. Yang, and H.-C. Lin, "Applications of novel dithienothiophene- and 2,7-carbazole-based conjugated polymers with surface-modified ZnO nanoparticles for organic photovoltaic cells," *Thin Solid Films*, vol. 519, no. 15, pp. 5212–5218, 2011.

[106] S. Shao, F. Liu, G. Fang, B. Zhang, Z. Xie, and L. Wang, "Enhanced performances of hybrid polymer solar cells with p-methoxybenzoic acid modified zinc oxide nanoparticles as an electron acceptor," *Organic Electronics*, vol. 12, no. 4, pp. 641–647, 2011.

[107] K. Yuan, F. Li, L. Chen, Y. Li, and Y. Chen, "Liquid crystal helps ZnO nanoparticles self-assemble for performance improvement of hybrid solar cells," *Journal of Physical Chemistry C*, vol. 116, no. 10, pp. 6332–6339, 2012.

[108] D. I. Son, B. W. Kwon, J. D. Yang, D. H. Park, B. Angadi, and W. K. Choi, "High efficiency ultraviolet photovoltaic cells based on ZnO-C_{60} core-shell QDs with organic-inorganic multilayer structure," *Journal of Materials Chemistry*, vol. 22, no. 3, pp. 816–819, 2012.

[109] C.-T. Chen, F.-C. Hsu, S.-W. Kuan, and Y.-F. Chen, "The effect of C_{60} on the ZnO-nanorod surface in organicinorganic hybrid photovoltaics," *Solar Energy Materials and Solar Cells*, vol. 95, no. 2, pp. 740–744, 2011.

[110] K. Yao, L. Chen, Y. Chen, F. Li, and P. Wang, "Interfacial nanostructuring of ZnO nanoparticles by fullerene surface functionalization for "Annealing-Free" hybrid bulk heterojunction solar cells," *Journal of Physical Chemistry C*, vol. 116, no. 5, pp. 3486–3491, 2012.

[111] B. Park, J.-H. Lee, M. Chang, and E. Reichmanis, "Exciton dissociation and charge transport properties at a modified donor/acceptor interfacepoly(3-hexylthiophene)/Thiol-ZnO bulk heterojunction interfaces," *Journal of Physical Chemistry C*, vol. 116, no. 6, pp. 4252–4258, 2012.

[112] A. J. Said, G. Poize, C. Martini et al., "Hybrid bulk heterojunction solar cells based on P3HT and porphyrin-modified ZnO nanorods," *Journal of Physical Chemistry C*, vol. 114, no. 25, pp. 11273–11278, 2010.

[113] S. Zhang, P. W. Cyr, S. A. McDonald, G. Konstantatos, and E. H. Sargent, "Enhanced infrared photovoltaic efficiency in PbS nanocrystal/semiconducting polymer composites: 600-fold increase in maximum power output via control of the ligand barrier," *Applied Physics Letters*, vol. 87, no. 23, Article ID 233101, 3 pages, 2005.

[114] K. M. Noone, E. Strein, N. C. Anderson, P.-T. Wu, S. A. Jenekhe, and D. S. Ginger, "Broadband absorbing bulk heterojunction photovoltaics using low-bandgap solution-processed quantum dots," *Nano Letters*, vol. 10, no. 7, pp. 2635–2639, 2010.

[115] J. Seo, M. J. Cho, D. Lee, A. N. Cartwright, and P. N. Prasad, "Efficient heterojunction photovoltaic cell utilizing nanocomposites of lead sulfide nanocrystals and a low-bandgap polymer," *Advanced Materials*, vol. 23, no. 34, pp. 3984–3988, 2011.

[116] W. Ma, S. L. Swisher, T. Ewers et al., "Photovoltaic performance of ultrasmall PbSe quantum dots," *ACS Nano*, vol. 5, no. 10, pp. 8140–8147, 2011.

[117] A. H. Ip, S. M. Thon, S. Hoogland et al., "Hybrid passivated colloidal quantum dot solids," *Nat Nano*, vol. 7, pp. 577–582, 2012.

[118] J. Xu, J. Wang, M. Mitchell et al., "Organic-inorganic nanocomposites via directly grafting conjugated polymers onto quantum dots," *Journal of the American Chemical Society*, vol. 129, no. 42, pp. 12828–12833, 2007.

[119] P. A. van Hal, M. M. Wienk, J. M. Kroon et al., "Photoinduced electron transfer and photovoltaic response of a MDMO-PPV:TiO_2 bulk-heterojunction," *Advanced Materials*, vol. 15, no. 2, pp. 118–121, 2003.

[120] W. J. E. Beek, L. H. Slooff, M. M. Wienk, J. M. Kroon, and R. A. J. Janssen, "Hybrid solar cells using a zinc oxide precursor and a conjugated polymer," *Advanced Functional Materials*, vol. 15, no. 10, pp. 1703–1707, 2005.

[121] D. J. D. Moet, L. J. A. Koster, B. De Boer, and P. W. M. Blom, "Hybrid polymer solar cells from highly reactive diethylzinc: MDMO-PPV versus P3HT," *Chemistry of Materials*, vol. 19, no. 24, pp. 5856–5861, 2007.

[122] S. Dayal, N. Kopidakis, D. C. Olson, D. S. Ginley, and G. Rumbles, "Direct synthesis of CdSe nanoparticles in poly(3-hexylthiophene)," *Journal of the American Chemical Society*, vol. 131, no. 49, pp. 17726–17727, 2009.

[123] L. H. Slooff, J. M. Kroon, J. Loos, M. M. Koetse, and J. Sweelssen, "Influence of the relative humidity on the performance of polymer/TiO_2 photovoltaic cells," *Advanced Functional Materials*, vol. 15, no. 4, pp. 689–694, 2005.

[124] S. D. Oosterhout, M. M. Wienk, M. Al-Hashimi, M. Heeney, and R. A. J. Janssen, "Hybrid polymer solar cells from zinc oxide and poly(3-hexylselenophene)," *Journal of Physical Chemistry C*, vol. 115, no. 38, pp. 18901–18908, 2011.

[125] S. Dowland, T. Lutz, A. Ward et al., "Direct growth of metal sulfide nanoparticle networks in solid-state polymer films for hybrid inorganic-organic solar cells," *Advanced Materials*, vol. 23, no. 24, pp. 2739–2744, 2011.

[126] A. Watt, E. Thomsen, P. Meredith, and H. Rubinsztein-Dunlop, "A new approach to the synthesis of conjugated polymer-nanocrystal composites for heterojunction optoelectronics," *Chemical Communications*, vol. 10, no. 20, pp. 2334–2335, 2004.

[127] J. H. Warner and A. A. R. Watt, "Monodisperse PbS nanocrystals synthesized in a conducting polymer," *Materials Letters*, vol. 60, no. 19, pp. 2375–2378, 2006.

[128] A. A. R. Watt, D. Blake, J. H. Warner et al., "Lead sulfide nanocrystal: conducting polymer solar cells," *Journal of Physics D*, vol. 38, no. 12, pp. 2006–2012, 2005.

[129] L. Chen, X. Pan, D. Zheng et al., "Hybrid solar cells based on P3HT and Si@MWCNT nanocomposite," *Nanotechnology*, vol. 21, no. 34, Article ID 345201, 2010.

[130] J. M. Lee, B. H. Kwon, H. I. Park et al., "Exciton dissociation and charge-transport enhancement in organic solar cells with quantum-Dot/N-doped CNT hybrid nanomaterials," *Advanced Materials*, vol. 25, no. 14, pp. 2011–2017, 2013.

[131] T.-H. Kim, S.-J. Yang, and C.-R. Park, "Carbon nanomaterials in organic photovoltaic cells," *Carbon Letters*, vol. 12, pp. 194–206, 2011.

[132] Q. Zheng, G. Fang, F. Cheng et al., "Hybrid graphene–ZnO nanocomposites as electron acceptor in polymer-based bulk-heterojunction organic photovoltaics," *Journal of Physics D*, vol. 45, Article ID 455103, 2012.

[133] C. X. Guo, H. B. Yang, Z. M. Sheng, Z. S. Lu, Q. L. Song, and C. M. Li, "Layered graphene/quantum dots for photovoltaic devices," *Angewandte Chemie*, vol. 49, no. 17, pp. 3014–3017, 2010.

[134] H. Derbal-Habak, C. Bergeret, J. Cousseau, and J. M. Nunzi, "Improving the current density Jsc of organic solar cells P3HT: PCBM by structuring the photoactive layer with functionalized SWCNTs," *Solar Energy Materials and Solar Cells*, vol. 95, no. 1, pp. S53–S56, 2011.

[135] D. Wang, J. K. Baral, H. Zhao et al., "Controlled fabrication of pbs quantum-dot/carbon-nanotube nanoarchitecture and its significant contribution to near-infrared photon-to-current conversion," *Advanced Functional Materials*, vol. 21, no. 21, pp. 4010–4018, 2011.

[136] Y. Jia, A. Cao, X. Bai et al., "Achieving high efficiency silicon-carbon nanotube heterojunction solar cells by acid doping," *Nano Letters*, vol. 11, no. 5, pp. 1901–1905, 2011.

[137] F. Li, Y. Shi, K. Yuan, and Y. Chen, "Fine dispersion and self-assembly of ZnO nanoparticles driven by P3HT-b-PEO diblocks for improvement of hybrid solar cells performance," *New Journal of Chemistry*, vol. 37, article 195, 2013.

[138] F. Li, W. Chen, and Y. Chen, "Mesogen induced self-assembly for hybrid bulk heterojunction solar cells based on a liquid crystal D-A copolymer and ZnO nanocrystals," *Journal of Materials Chemistry*, vol. 22, no. 13, pp. 6259–6266, 2012.

[139] K. Yuan, F. Li, Y. Chen, X. Wang, and L. Chen, "In situ growth nanocomposites composed of rodlike ZnO nanocrystals arranged by nanoparticles in a self-assembling diblock copolymer for heterojunction optoelectronics," *Journal of Materials Chemistry*, vol. 21, no. 32, pp. 11886–11894, 2011.